

Characterisation of CIP29: a potential target of the eukaryotic DNA damage response

Alice Armstrong

MSc by Research

Lancaster University

August 2016

I, Alice Armstrong, confirm that the work presented in this thesis is my own and has not been submitted in substantially the same form for the award of a higher degree elsewhere. Where information has been derived from other sources I confirm that this has been indicated in the thesis.

Alice Armstrong

Characterisation of CIP29: a potential target of the eukaryotic DNA damage response.

MRes

August 2016

Abstract

Cytokine Induced Protein 29 (CIP29) was originally identified as protein over-expressed in hepatocellular carcinoma, and expression of the protein has since been found to be upregulated in multiple other cancers (Fukuda et al, 2002; Leaw et al, 2004). Several potential roles have been proposed for CIP29. It has been suggested that the protein plays a role in cellular proliferation, perhaps through cell cycle regulation (Fukuda et al, 2002). Additionally, studies have suggested that CIP29 may be an RNA binding protein (RBP) involved in mRNA export (Dufu et al, 2010). Previous research by this laboratory found that the *X.laevis* ortholog of CIP29, XCip29, is phosphorylated in response to DNA double strand breaks (DSBs). This phosphorylation was shown to be dependent on the activity of ATM, one of the three PI3KK kinases that orchestrate the DNA damage response (DDR).

The purpose of our research was to investigate the function of the human CIP29 protein and to explore a potential role for the protein in the cellular response to DNA damage. DNA-damage dependent phosphorylation of human CIP29 could not be detected in this study. CRISPR genome editing was used to generate two CIP29 mutant cell lines, named C9 and C60. The C60 cells were shown to express a mutant form of the CIP29 protein, in which the SAP domain was deleted, whilst in the C9 cells, expression of CIP29 is effectively abolished.

Both cell lines demonstrated reduced proliferation in comparison with wild-type cells, with the defect in the C9 cells more pronounced. FACS analysis revealed a slightly reduced proportion of the C60 cells in the S and G2/M phases of the cell cycle compared to wild-type cells, which could account for the slightly reduced proliferation rate seen in these cells. FACS analysis performed on the C9 cells revealed evidence of a cytokinesis defect, implicating the CIP29 protein in cytokinesis. In order to further investigate the potential involvement of CIP29 in the DDR, sensitivity assays using DSB-inducing agents were performed. These assays

did not reveal any increased sensitivity of either the C9 or C60 cells to the drugs, indicating that CIP29 may not play a role in the DDR to DSBs.

Table of Contents

Abstract	2
Table of Contents	3
List of Figures	5
List of Tables	6
Abbreviations	7
Acknowledgments	9
Chapter 1: Introduction	10
1.1 Double strand break (DSB) repair	13
1.2 The ATM protein kinase	13
1.3 RNA processing and the DNA damage response	17
1.4 CIP29	25
1.5 This Thesis	31
Chapter 2: Materials and Methods	Error! Bookmark not defined.
2.1: Molecular Biology Techniques	33
2.1.1: Restriction digests	34
2.1.2: Polymerase Chain Reaction (PCR)	34
2.1.3: Purification of PCR products using the QIAquick® PCR Purification Kit	35
2.1.4: Ethanol precipitation of PCR products	35
2.1.5: A-tailing of PCR products	35
2.1.6: Gel Electrophoresis	35
2.1.7: QIAquick Gel Extraction	36
2.1.8: Ligation	36
2.1.9: Transformation of plasmids into chemically competent E.coli DH5a cells	36
2.1.10: Alkaline lysis miniprep method	36
2.1.11: QIAGEN® Miniprep method	36
2.1.12: QIAGEN® Midiprep method	37
2.1.13: Preparation of genomic DNA	37
2.2: Protein Methods:	37

2.2.1: Preparation of total cell extracts	37
2.2.2: Bradford assay method.....	38
2.2.3: SDS-PAGE Electrophoresis.....	38
2.2.4: Western blotting.....	39
2.2.5: Staining the nitrocellulose membrane with antibody	40
2.2.6: Developing Western Blots by Enhanced Chemiluminescence (ECL)	40
2.2.7: Stripping Western Blots	40
2.3: Cell Culture Techniques	41
2.3.1. Cell culture conditions	41
2.3.2. Plasmid Transfection.....	41
2.3.3 Metabolic Proliferation assay.....	42
2.3.4 Cytotoxicity Assay.....	42
2.3.5 Clonogenic survival assay.....	42
2.3.6 Chromosome spreading	43
2.3.7 Fluorescent Advanced Cell Sorting (FACS)	43
Chapter 3: Results.....	45
3.1: Phosphorylation of CIP29	45
3.1.1. Analysis of CIP29 in response to double-strand breaks.....	45
3.1.2. Phosphorylation of XCip29 in human cells.....	46
3.2. Characterisation of CIP29 Knockout cells	47
3.2.1. Generation of CIP29 mutant cells by CRISPR cloning	47
3.2.2. Absence of CIP29 expression in the CIP29 mutant cell lines, C9 and C60	50
3.2.3. Sequencing of the CIP29 mutant cell lines.....	50
3.2.4. Assessment of CIP29 mutant cell proliferation	55
3.2.5 Metaphase spread analysis of CIP29 mutant cell lines.....	56
3.2.6. Cell cycle analysis of CIP29 mutant cells.....	60
3.2.7. Sensitivity of CIP29 mutant cells to etoposide and camptothecin	62
3.2.8. Sensitivity of CIP29 Knockout cells to Neocarzinostatin.....	64
3.2.9 Generation of CIP29 stable transfectant cell lines	65
Chapter 4: Discussion.....	66
4.1: DNA-damage dependent phosphorylation of CIP29 in human cells.....	67
4.2: Confirmation of CIP29 mutated cell lines	68
4.3: Proliferation and cell cycle progression of the CIP29 mutant cell lines	69
4.4: Sensitivity of the knockout cell lines to DNA-damaging agents.....	73

4.5: Conclusion.....	73
References.....	75

List of Figures

Fig 1.1 Diagram illustrating the DDR network.

Fig 1.2 Diagram demonstrating the activation of ATM by DNA DSBs and the subsequent phosphorylation of multiple downstream effector proteins.

Fig 1.3 The formation of an R-loop.

Fig 1.4 Diagram demonstrating the process of mRNA splicing and how it can be used to produce several differing proteins from the same gene sequence.

Fig 1.5 Diagram demonstrating the process of mRNA export from the nucleus.

Fig 1.6 Diagram demonstrating the sequence alignment of CIP29 in humans, mice, chickens and frogs.

Fig 1.7 Phosphorylation of XCip29 in Xenopus egg extract in the presence of linear dsDNA.

Fig 1.8 Phosphorylation of XCip29 is dependent upon ATM activity.

Fig 3.1 Western blots of untreated, and H₂O₂ and NCS treated MRC5-V1 cell extracts following resolution by A) normal SDS-Page or B) Phos-Tag™ gel electrophoresis.

Fig 3.2 Western blots of MRC5-V1 cells transfected with XCip29 PCI-FF and incubated in the presence or absence of caffeine.

Fig 3.3 Diagram demonstrating the principles of CRISPR-Cas genome editing.

Fig 3.4 CIP29 genomic DNA surrounding exon 2 shown from PCR primer EP42 to PCR primer EP41.

Fig 3.5 Western blots of MRC5-V1, C9 and C60 cell extracts, incubated with CIP29 and GAPDH.

Fig 3.6 MRC5-V1, C9 and C60 genomic DNA run on a 0.8% agarose gel, alongside a 1kB marker.

Fig 3.7 Agarose gel images of: A) The negative control, MRC5-V1 C9 and C60 PCR products and B) The C60 lower band and higher band products.

Fig 3.8 Genomic DNA of the C60 cell line from PCR primer EP42 to PCR primer EP41.

Fig 3.9 Diagram showing the amino acid sequence of CIP29.

Fig 3.10 Section of the gene sequence from the wild-type MRC5 cells, and the two 940bp C60 plasmids , HB1 and HB2.

Fig 3.11 The amino acid sequence of wild-type CIP29 exon 2, and the amino acid sequences of the two CRISPR generated C60 fragments, HB1 and HB2.

Fig 3.12 Graph showing the proliferation rates of MRC5-V1, C9 and C60 cells over 4 days.

Fig 3.13 Images showing examples of open and closed arm phenotypes from the MRC5-V1, C9 and C60 cell lines.

Fig 3.14 The results from FACS analysis carried out on the MRC5-V1, C9 and C60 cell lines.

Fig 3.15 Graph showing the sensitivity of MRC5-V1 C9 and C60 cells to camptothecin (0-1000nM).

Fig 3.16 Graph showing the sensitivity of MRC5-V1,C9 and C60 cells to etoposide (0-20 μ M).

Fig 3.17 Graph showing the sensitivity of MRC5-V1, C9 and C60 cells to NCS, established by a clonogenic survival assay.

List of Tables

Table 2.1 Composition of buffers and solutions used in this work.

Table 2.2 PCR primers

Table 2.3 Recipes for 10ml of resolving gel for SDS-PAGE.

Table 2.4 Recipe for 3ml of stacking gel for SDS-PAGE.

Table 2.5 Recipe for 6ml of Phos-Tag™, 8% w/v acrylamide resolving gel.

Table 2.6 The primary antibodies used in this work.

Table 3.1 Table showing the average number of metaphases per field, and the average degree of chromosome spread, for each chromosome spreading technique.

Table 3.2 Table showing the number of open and closed arm phenotypes observed in 200 metaphases from the MRC5-VI, C9 and C60 cell lines.

Abbreviations

ABL1	ABL proto-oncogene 1
APC/C	Anaphase-promoting complex/cyclosome
ATM	Ataxia Telangiectasia Mutated
ATP	Adenosine triphosphate
ATR	Ataxia Telangiectasia and Rad 3 related protein
ATRIP	ATR Interacting Protein
BACH1	BTB domain and CNC homolog 1
BCLAF1	BCL2 associated transcription factor 1
BER	Base Excision Repair
BLM	Bloom syndrome protein
BRCA1	Breast cancer type 1 susceptibility protein
Cas9	CRISPR associated protein 9
Cdc	Cell division cycle
Cdk	Cyclin dependent kinase
Cep63	Centrosomal protein of 63kDa
Chk1	Checkpoint kinase 1
Chk2	Checkpoint kinase 2
CIP29	Cytokine Induced Protein 29
CPT	Camptothecin
CRISPR	Clustered Regularly Interspaced Short Palindromic Repeats
CtIP	CtBP-interacting protein
DAPI	4'6-diamidino-2-phenylindole
dATP	Deoxyadenosine triphosphate
DDR	DNA damage response
DMEM	Dulbecco's Modified Eagle Medium
DMSO	Dimethyl sulfoxide
DNA	Deoxyribonucleic acid
DNA-PKcs	DNA dependent protein kinase catalytic subunit
dNTPs	Deoxynucleotide Triphosphate
DSB	Double Strand Break
dsDNA	Double-stranded DNA
ECL	Electrochemicaluminescence
EDTA	Ethylenediaminetetraacetic acid
Epo	Erythropoietin
EWS	Ewing sarcoma RNA binding protein 1
EXO1	Exonuclease 1
FA	Fanconi Anaemia
FACS	Fluorescence-activated cell sorting
FANC	Fanconi Anaemia Complementation Group
Fen1	Flap structure-specific endonuclease 1
FMR1	Fragile X Mental Retardation 1
FUS	Fused in Sarcoma
FXN	Friedrich Ataxia Protein
GAPDH	Glyceraldehyde 3-phosphate dehydrogenase
H2AX	H2A (Histone Family Member X)
Hcc-1	Hepatocellular carcinoma-1
HEK	Human Embryonic Kidney
HnRNPUL	Heterogeneous nuclear ribonucleoprotein U-like protein

HR	Homologous Recombination
HRP	Horseradish Peroxidase
IR	Ionizing radiation
KCl	Potassium Chloride
kDa	kilodalton
MAP4K2	Mitogen-Activated Protein kinase kinase kinase kinase 2
Mdm2	Mouse double minute 2 homolog (MDM2)
MgcRacGAP	Rac GTPase-activating protein 1
MGMT	O ⁶ -alkylguanine DNA alkyltransferase
MKLP	Mitotic kinesin-like protein
MMR	Mismatch Repair
MRN	Mre11-Rad50-Nbs1
mRNA	Messenger Ribonucleic acid
mRNP	Messenger ribonucleoprotein
MSH2	MutS protein homolog 2
NAPDH	Nicotinamide adenine dinucleotide phosphate
NCS	Neocarzinostatin
NER	Nucleotide Excision Repair
NHEJ	Non-homologous end-joining
Noxa	Phorbol-12-myristate-13-acetate induced protein 1
NPC	Nuclear Pore Complex
p15	Also known as CDKN2B (cyclin dependent kinase inhibitor 2B)
p53	Phosphoprotein p53
PARP1	Poly (ADP-Ribose) Polymerase I
PBS	Phosphate-buffered saline
PCR	Polymerase Chain Reaction
PI3KK	Phosphatidylinositol-3-OH kinase-related kinase
Plk1	Polo-like kinase 1
PMSCS	Premature Sister Chromatid Separation
Prp	Pre-Mrna-processing
Puma	P53-upregulated modulator of apoptosis
RAD51	DNA repair protein RAD51 homolog 1
RBP	RNA binding protein
RGEN	RNA-guided engineered nucleases
RhoA	Ras homolog gene family, member A
RNA	Ribonucleic acid
RNAPII	RNA Polymerase II
ROS	Reactive Oxygen Species
RPA	Replication Protein A
SAC	Spindle Assembly Checkpoint
SDS-PAGE	Sodium dodecyl sulphate polyacrylamide gel electrophoresis
Ser	Serine
SF3B1	Splicing factor 3B subunit 1
SiRNA	Small Interfering Ribonucleoprotein
SSB	Single strand break
ssDNA	Single-stranded DNA
Sub2	Suppressor of Brr1 protein 2
Tap	Transporter associated with antigen processing
TREX	Transcription-Export complex
U2AF	U2 Auxillary Factor 35/65

UAP56	Also known as DDX39B, DEAD-box Helicase 39B
URH49	Also known as DDX39A, DEAD-box Helicase 39A
UV	Ultra-violet
V (D) J	Variable (Diversity) Joining
XCip29	X.laevis Cytokine Induced Protein 29
XPC	Xeroderma pigmentosum, complementation group C
XPF	Xeroderma pigmentosum, complementation group F
XPG	Xeroderma pigmentosum complementation group G

Acknowledgments

I would like to acknowledge the help of my MRes supervisor Dr Elaine Taylor, whose guidance and support throughout my laboratory research and thesis writing has been invaluable, for which I am very grateful. I would also like to express my gratitude to my second supervisor, Dr Howard Lindsay, for his helpful advice and support in the laboratory.

Chapter 1: Introduction

When eukaryotic cells divide, they accurately duplicate their genome, and then subsequently divide the genome equally between two new daughter cells. The intention is to produce two new cells, each with identical genomic material to the parent cell, but this does not always occur. Occasionally, cell division may fail, or a high frequency of errors may arise during the process, leading to genomic alterations in the daughter cells, such as mutations to specific genes, gene amplifications, and loss, gain, or rearrangement of chromosomes. DNA damage-induced genomic alterations may arise from multiple sources, both endogenous, and exogenous to the cell (Shen, 2011). Endogenous sources include base-pair mismatching occurring during DNA replication, and exposure to the reactive oxygen species (ROS) produced during normal cellular metabolism. Causes of exogenous DNA damage include ultraviolet (UV) and ionizing radiation (IR), cigarette smoke, and treatment with chemotherapeutic agents (Boucas et al, 2012; Dutertre et al, 2014; Mills et al, 2003). An increased propensity for alterations to the genome during the cell cycle is termed genomic instability and has been implicated in the pathogenesis of many human diseases, including neurodegenerative disorders, immune deficiencies, infertility, and cancer (Dutertre et al, 2014; Shen, 2011).

Fortunately, eukaryotic cells have evolved a means of combating assaults to their genomic integrity: a complex global signalling network known as the DNA damage response (DDR). Fundamentally, the DDR is a signal transduction pathway consisting of sensors, which recognize the DNA damage, transducers, which relay the nature of the damage and activate the appropriate downstream target proteins, and effectors, which implement cellular processes to resolve the damage, or otherwise ameliorate its consequences (Jackson & Bartek, 2009). Initially, the DNA damage must be recognized by sensor proteins, such as Mre11-Rad50-Nbs1 (MRN) complex, and poly (ADP-ribose) polymerase 1 (PARP1) (Rupnik et al, 2010; Stilmann et al, 2009). Typically, these sensor proteins then recruit one or more of the three upstream DNA kinases, Ataxia Telangiectasia Mutated (ATM), Ataxia Telangiectasia and Rad 3 related protein (ATR) and DNA-dependent protein kinase, (DNA-PKcs), to the site of the DNA assault. ATM and ATR are the 'master transducers': they directly stimulate phosphorylation of hundreds of downstream DDR proteins, but also instigate indirect protein phosphorylation by activating secondary protein kinases such as Chk1 and Chk2 (Marechal & Zou, 2013). ATM is chiefly activated in response to DNA double-strand breaks

(DSBs), whereas ATR responds to several forms of DNA damage, such as replication fork stalling, inter-strand cross-linking, and oxidative base damage (Cortez, 2005; Marechal & Zou, 2013). Conversely, DNA-PKcs has a lesser number of downstream target proteins, and functions primarily in the coordination of non-homologous end joining for DNA DSB repair (Marechal & Zou, 2013).

The downstream 'effector' DDR proteins execute a number of cellular mechanisms in response to DNA damage, such as activation of the DNA repair pathways, cell cycle arrest and regulation of gene expression. If the DNA damage is deemed irreparable, the DDR can then target the cell for apoptosis.

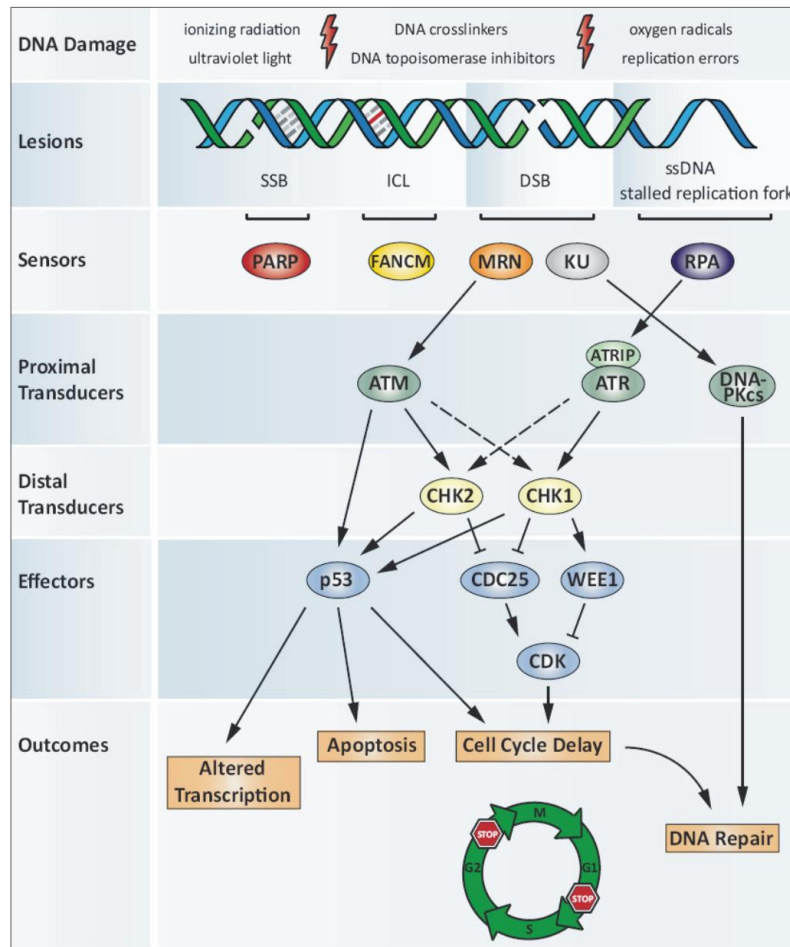


Fig 1.1 Diagram demonstrating the workings of the DDR. DNA damage lesions are recognised by sensors, which then activate the PI3KK kinases, ATM, ATR and DNA-PKcs. These kinases then activate downstream effector proteins, either directly or through secondary kinases. These effectors then execute a number of mechanisms to repair the DNA lesions, or otherwise lessen their impact on genomic instability.

Image Citation: Targeting DNA double-strand break signalling and repair: recent advances in cancer therapy

Daniela Hühn, Hella A. Bolck, Alessandro A. Sartori

Institute of Molecular Cancer Research, University of Zurich, Switzerland

Swiss Med Wkly. 2013;143:w13837 www.smw.ch

Image Reproduced with the permission of Swiss Medical Weekly

The DDR includes an arsenal of DNA repair pathways, each designed to repair specific types of DNA lesion. The major pathways include: mismatch repair (MMR), to correct base-pairing errors in newly replicated DNA, base excision repair (BER), to repair damage to individual DNA bases, nucleotide excision repair (NER), to repair lesions either distorting the DNA double helix, or blocking DNA replication/transcription, and homologous recombination (HR) and non-homologous end joining (NHEJ), to repair DSBs.

1.1 Double strand break (DSB) repair

DNA DSBs, i.e. lesions in which both strands of the DNA duplex have been severed, are common, and arguably the most dangerous form of DNA lesion, as not only can a single DSB prove lethal to a cell, but they can also result in chromosomal rearrangements which trigger tumorigenesis. The primary exogenous causes of DSBs are exposure to ionizing radiation, chiefly gamma rays and X-rays, and treatment with certain chemotherapeutic agents (Khanna & Jackson, 2001). The endogenously generated ROS typically generates single-stranded DNA breaks, but DSBs may arise if two of these single-stranded breaks occur in close proximity on opposing DNA strands (Lieber, 2010). Stalling of the replication fork on its progression along the DNA strand, which can be caused by a variety of DNA lesions and replicative stresses, can also lead to double-strand breakage (Khanna & Jackson, 2001). Additionally, abortive activity of the type II Topoisomerase enzymes, which break the phosphate backbone of the DNA double helix during replication, can induce DSBs, as can DNA replication occurring across a nick (Lieber, 2010). Physical stress on the DNA duplex, due to defective telomere processing, is a further cause of DSBs (Murnane, 2006).

Intentional DNA DSBs can arise during the processes of V(D)J recombination and immunoglobulin class-switch recombination, which are crucial to the maturation of B and T lymphocytes (Khanna & Jackson, 2001) and also, in meiotic cells where the primary inducer of DSBs, a topoisomerase IV-like protein, Spo11, induces DSBs in order to allow crossover between homologous chromosomes during the prophase I stage of meiosis (Cao et al).

Two distinct repair pathways co-ordinate with one another to repair DNA DSBs. Non-homologous end-joining (NHEJ) is the principal DNA re-joining pathway and can occur in all stages of the cell cycle. In NHEJ, the broken DNA ends are processed, and ligated together in a non-conservative fashion, with potential for mutagenesis. In comparison, homologous recombination (HR), which is solely employed during the late S and G2 phases of the cell cycle, uses a homologous sister chromatid as a template for DSB repair, and is a conservative and predominantly error-free pathway (Krajewska et al, 2015).

1.2 The ATM protein kinase

The cellular response to DNA DSBs is dependent upon DDR signalling by the ATM protein kinase. Along with the two other major protein kinases, ATR and DNA-PKcs, ATM is a member of the phosphatidylinositol-3-OH kinase-related kinase (PI3KK) family. Following recognition of a DSB by the sensor MRN complex, ATM is recruited to the lesion site, whereupon it is rapidly activated by autophosphorylation (Bakkenist & Kastan, 2003). ATM then amplifies the DSB signal by phosphorylating the secondary protein kinase Chk2, and also all three members of the MRN complex itself (Chaudhary & Al-Baradie, 2014; Lavin et al, 2015). A plethora of effector proteins, each with specific roles in either repairing, or mitigating the consequences of the DSB, are then phosphorylated, either directly by ATM, or through Chk2 activity (see fig 1.2). An early vital stage in DSB repair is the phosphorylation of H2AX to γ H2AX, which then facilitates the accumulation of other repair proteins at the DSB site (Rogakou et al, 1998). ATM phosphorylates proteins directly involved in homologous recombination, such as BRCA1, BLM, and CtIP, and can also directly phosphorylate DNA-PKcs, which then co-ordinates NHEJ repair (Chen et al, 2007; Shiloh, 2003).

In order to allow sufficient time for DSB repair to occur, ATM can initiate several cell cycle checkpoints: molecular signalling cascades designed to promote cell cycle arrest at specific stages in the cell cycle. Activation of the G1/S cell cycle checkpoint prevents replication of cells harbouring damaged DNA, the intra-S checkpoint can halt DNA replication itself, and the G2/M checkpoint prevents damaged cells from undergoing mitosis. (Bartek et al, 2004; Kastan et al, 1992; Matsuoka et al, 1998). Cell cycle checkpoint arrest occurs through the inhibition of Cdk-cyclin complexes, which normally promote cell cycle progression. For example, in response to DNA damage, ATM phosphorylates Chk2, which in turn phosphorylates the regulatory subunit Cdc25A. Cdc25A activation leads to the sustained phosphorylation and inactivation of the Cdk2-cyclin E complex, halting the cell cycle at the G1/S checkpoint (Falck et al, 2001).

If the DNA damage sustained is irreparable, the ATM phosphorylation target p53 can then orchestrate apoptotic cell death, through transcriptional regulation of pro-apoptotic and anti-apoptotic genes (Roos & Kaina, 2013).

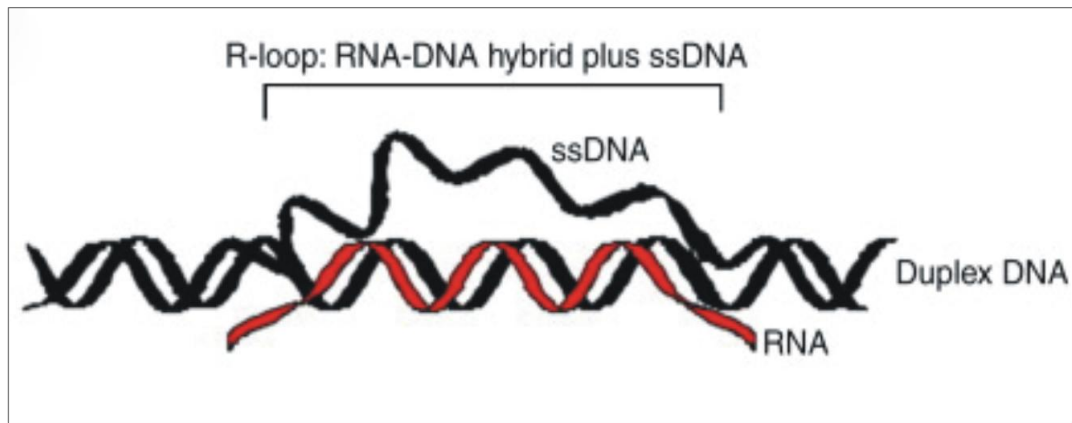


Fig 1.3 The formation of an R-loop.

The nascent RNA strand has hybridized with the template DNA strand, producing an RNA: DNA hybrid, and a single strand of DNA. Image Citation: Ivancic-Bace, I., et al. (2012). "Tuning in to interference: R-loops and cascade complexes in CRISPR immunity." *J Mol Biol* 422(5): 607-616.

Image reproduced with the permission of Elsevier.

R-loops have been shown to perform a variety of physiological roles in cells, such as regulating gene expression (Ginno et al, 2012; Skourti-Stathaki et al, 2014), DNA replication (Kogoma, 1997), Ig class switch recombination (Chaudhuri & Alt, 2004), and DNA repair (Keskin et al, 2014). Whilst these programmed R-loops do not appear to lead to DNA damage, unscheduled or excessive formation of R-loops can result in various forms of genomic instability. For example, the ssDNA that is exposed during R-loop formation is vulnerable to base modifications (Basu et al, 2011). DNA DSBs can arise through processing of R-loops by the NER endonucleases XPF and XPG (Sollier et al, 2014), and through collision between R-loops and replication machinery (Gan et al, 2011). These DSBs can lead to chromosomal translocations, causing tumorigenesis. Furthermore, epigenetic changes induced by R-loops have been shown to be implicated in the pathogenesis of the neurodegenerative diseases Friedrich's ataxia and Fragile X syndrome, through inhibiting the transcriptional activity of key genes, FMR1 in Friedrich's ataxia, and FXN in Fragile X syndrome (Groh et al, 2014).

Recently, ATM has been implicated in the DDR to R-loop formation. Tresini et al. found that ATM was phosphorylated in response to transcription blocking by R-loops, in the absence of DSBs. They hypothesized that ATM is involved in the chromatin displacement of splicing factors, which are involved in modulating gene expression by removing certain exons from the mRNA sequence (Dutertre et al, 2010). It is thought that the dissociation of groups of splicing factors (known as spliceosomes) from the transcription machinery allows backtracking of RNA Pol II, which is necessary for repair of the R-loop lesion (Tresini et al,

2015). Therefore, ATM assists not only in DSB repair, but also in the response to both oxidative DNA damage, and transcription blocking lesions such as R-loops.

It is clear that ATM is a multifunctional DDR protein, evidenced by its numerous described roles in the DDR, and the wide range of downstream ATM target proteins that have been identified thus far. The severe genomic instability that results from mutation of the ATM gene proves just how indispensable ATM is in mounting an effective DDR. Mutation of the ATM gene, located at 11q22-23, results in the syndrome Ataxia Telangiectasia (A-T), which has a wide breadth of clinical features relating to genomic instability, such as immunodeficiency, increased cancer predisposition, radiosensitivity, oculocutaneous telangiectasia, progressive cerebellar neurodegeneration, and gonadal dysgenesis. Despite improved management, the life expectancy for the disease is between the second and third decades of life (Chaudhary & Al-Baradie, 2014).

Recent research has suggested there is a still long way to go to uncover the full scope of ATM's involvement in the DDR. Research by Matsuoka et al. into the substrates of ATM and its fellow PI3KK-like kinase ATR and revealed an unprecedented number of downstream phosphorylation targets from these two kinases: between the two proteins, over 700 proteins appear to be phosphorylated in response to ionizing radiation. Of these 700 proteins, 421 were attributed a probable biological role. Of these, 48% were thought to be involved in nucleic acid metabolism, in processes such as DNA replication, DNA repair, chromatin packaging and remodelling, and mRNA processing and transcription. Other biological processes assigned to the proteins included protein metabolism and modification, cell cycle control, signal transduction, cell structure and motility, and cell proliferation and differentiation (Matsuoka et al, 2007). The extensive range of different cellular processes carried out by these downstream target proteins proves that significant future work will be required before we can fully comprehend all of the functions of ATM, and indeed the DDR network itself.

1.3 RNA processing and the DNA damage response

RNA processing refers to post-transcriptional covalent modifications made by RNA-binding proteins (RBPs) to an mRNA molecule to prepare it for translation (Luna et al, 2008). RBPs can exert control over transcription itself, including transcription elongation i.e. the regulated addition of nucleotides to the mRNA chain (Saunders et al, 2006), and transcription termination (Rosonina et al, 2006). During transcription, they can prevent the

formation of potentially damaging R-loops (Huertas & Aguilera, 2003). They mediate alternative mRNA splicing, in which the non-coding regions of DNA, or introns, are removed, and the exons joined together to form a continuous coding mRNA sequence (Fu & Ares, 2014). Both the 3' and 5' ends of the mRNA transcript can be modified by RBPs (Jurado et al, 2014). Eventually, the mRNA molecule is exported from the cell nucleus, whereupon translation occurs on a ribosome in the cell cytoplasm (Katahira, 2012).

In recent years, increasing attention has been given to examining the interplay between RNA processing and genomic stability. RNA processing factors have been consistently shown to be associated with the prevention of genomic instability (Aguilera, 2005; Chan et al, 2014; Gomez-Gonzalez et al, 2011; Paulsen et al, 2009; Santos-Pereira et al, 2014). In fact, studies have shown that almost every aspect of RNA processing is potentially mutable to a genome instability phenotype. (Jimeno et al, 2002; Li & Manley, 2005; Luna et al, 2005; Wellinger et al, 2006). Of late, research has focused specifically on the interaction between RNA processing and the DDR. Numerous large-scale proteomic and genomic screens have revealed that RBPs are activated by DDR proteins, including ATM and ATR, and PARP-1 (Kai, 2016; Matsuoka et al, 2007; Paulsen et al, 2009). The proteomic analysis of ATM and ATR substrates performed by Matsuoka et al. revealed an unexpected enrichment of RBPs involved in splicing, RNA modification and control of translation, indicating a more prominent role for RNA processing in the DDR than previously thought. (Matsuoka et al, 2007). Since then, many specific mechanisms by which RNA processing supports and adapts the DDR have been described, as outlined in these reviews (Dutertre et al, 2014; Montecucco & Biamonti, 2013; Naro et al, 2015; Wickramasinghe & Venkitaraman, 2016). Furthermore, several RBPs have been identified as having direct roles in the DDR (Adamson et al, 2012; Maréchal et al, 2014; Polo et al, 2012). The ways in which RNA processing functions to maintain genomic stability will be discussed below.

RBPs can modulate DDR gene expression:

One means by which RNA processing modulates the DDR is through the control of gene expression. Following DNA damage, gene expression is significantly reduced by global repression of transcription (Mayne & Lehmann, 1982), poly-adenylation of pre-mRNA (Kleiman & Manley, 2001), and translation (Deng et al, 2002). This is thought to occur to avoid collisions between repair and transcription machineries (Wickramasinghe & Venkitaraman, 2016). Amidst this global reduction in gene expression, it is essential that expression of DDR genes is not only maintained, but increased as appropriate. DDR gene

expression must be adapted for the particular DNA damage sustained. A variety of RNA processing mechanisms are involved in the regulation of DDR gene expression, such as transcription elongation, mRNA splicing and mRNA export (Wickramasinghe & Venkitaraman, 2016).

For example, following DNA damage, transcription elongation has been shown to be regulated by the Cdk-cyclin complex Cdk12-Cyclin K, through its phosphorylation of RNA Pol II. Depletion of the complex resulted in reduced expression of many DDR genes, including BRCA1, FANCI and ATR (Blazek et al, 2011). Lower amounts of RNAPII on the promoters of BRCA1, FANCI and ATR genes was observed, and the production of mRNA coding for these proteins was reduced, proving that a transcription defect was responsible for the decreased expression of these proteins. Depletion of the Cdk12-cyclin K complex also led to increased sensitivity to DNA damaging agents, such as etoposide, camptothecin and mitomycin C, proving its importance in preventing genomic instability (Blazek et al, 2011). The example of Cdk12-cyclin K attests to the role transcription regulation plays in mounting a proficient DDR.

RBPs can also regulate DDR gene expression through alternative mRNA splicing. In this process, particular exons i.e. the coding regions of an mRNA sequence, can be selectively included or excluded from the sequence. This allows a diverse range of proteins, with differing biological functions, to be produced from the same gene and can be used to adapt DDR gene expression to the specific type of damage sustained (Dutertre et al, 2010)

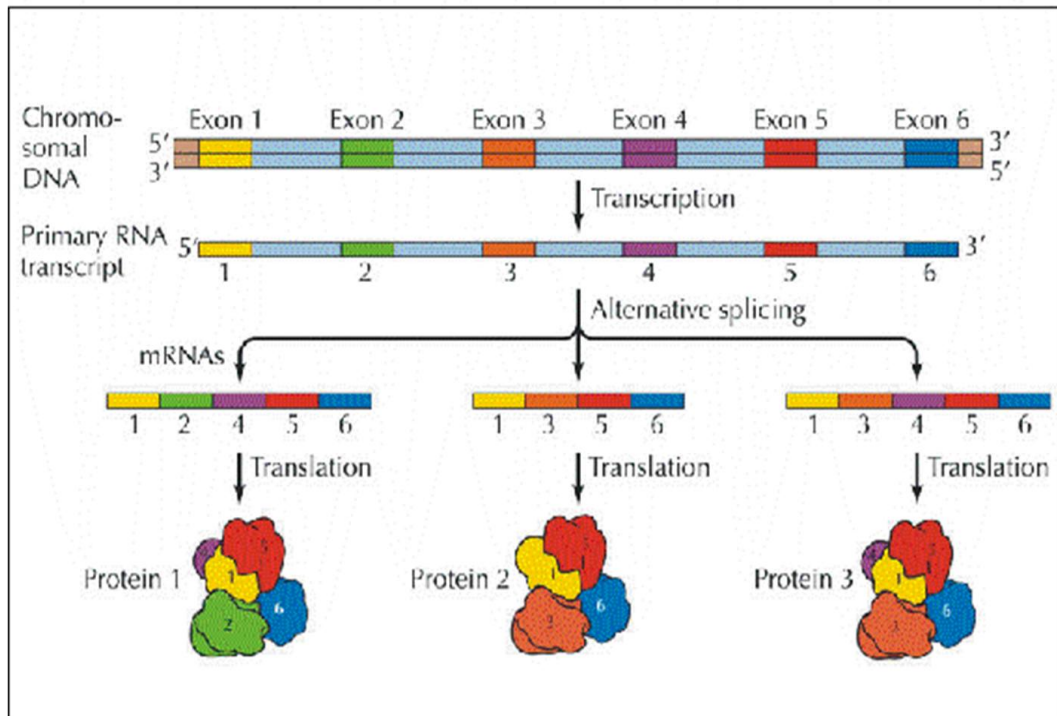


Fig 1.4 Diagram demonstrating the process of mRNA splicing and how it can be used to produce several differing proteins from the same gene sequence. Image Citation: THE CELL, Fourth Edition, Fig 5.5. © 2006 ASM Press and Snauer Associates, Inc.

Image reproduced with the permission of John Wiley and Sons.

mRNA splicing machinery is activated in response to DNA damage by BRCA1. BRCA1 is phosphorylated by both ATM and ATR, and appears to predominantly function as a scaffold protein, triggering the assembly of several multiprotein complexes with varying roles in the DDR, such as DSB repair by HR, and cell cycle checkpoint activation (Savage & Harkin, 2009). Phosphorylated BRCA1 has been shown to activate BCLAF1, which then mediates the formation of a complex of mRNA splicing proteins (including, Prp8, U2AF35/65 and SF3B1)(Savage et al, 2014). These proteins then promote the efficient splicing and stability of BRCA1 target proteins, such as ATRIP, BACH1 and EXO1. Depletion of BRCA1 and BCLAF1 was not only shown to substantially reduce expression of these three target proteins, but also increased sensitization of cells to both IR and the genotoxic drug etoposide, and inhibited DSB repair. Additionally, an increased incidence of chromosomal aberrations was observed when cells depleted of either BRCA1 or BCLAF1 were treated with IR.

A further example of mRNA splicing modulating DDR gene expression can be seen in the Ewing Sarcoma protein (EWS). EWS has been shown to regulate alternative splicing of mRNA produced from transcription of the Chek2 gene, which codes for the protein kinase Chk2, as well as the MAP4K2 and ABL1 genes (Paronetto et al, 2011). Knockdown of the protein was shown to result in considerably increased sensitivity to UV irradiation.

Additionally, RBPs can modulate gene expression via the sustained export of mRNAs coding for DDR proteins following damage. The Transcription-Export (TREX) complex, comprising the multimeric THO subcomplex and the proteins UAP56 and Aly, is responsible for mRNA export. The complex accompanies RNA polymerase II (RNA Pol II) along the DNA strand during transcription and coordinates packaging of the mRNA molecule and various associating factors into messenger ribonucleoprotein complexes (mRNPs) ready for export (Katahira, 2012). The mRNPs are then conveyed to the transport receptor Tap-p15, which facilitates export of the molecules through nuclear pore complexes (NPCs) in the nuclear envelope (Strasser et al, 2002). The TREX-2 complex assists with the transport of mRNPs through the nuclear pore complexes (Umlauf et al, 2013).

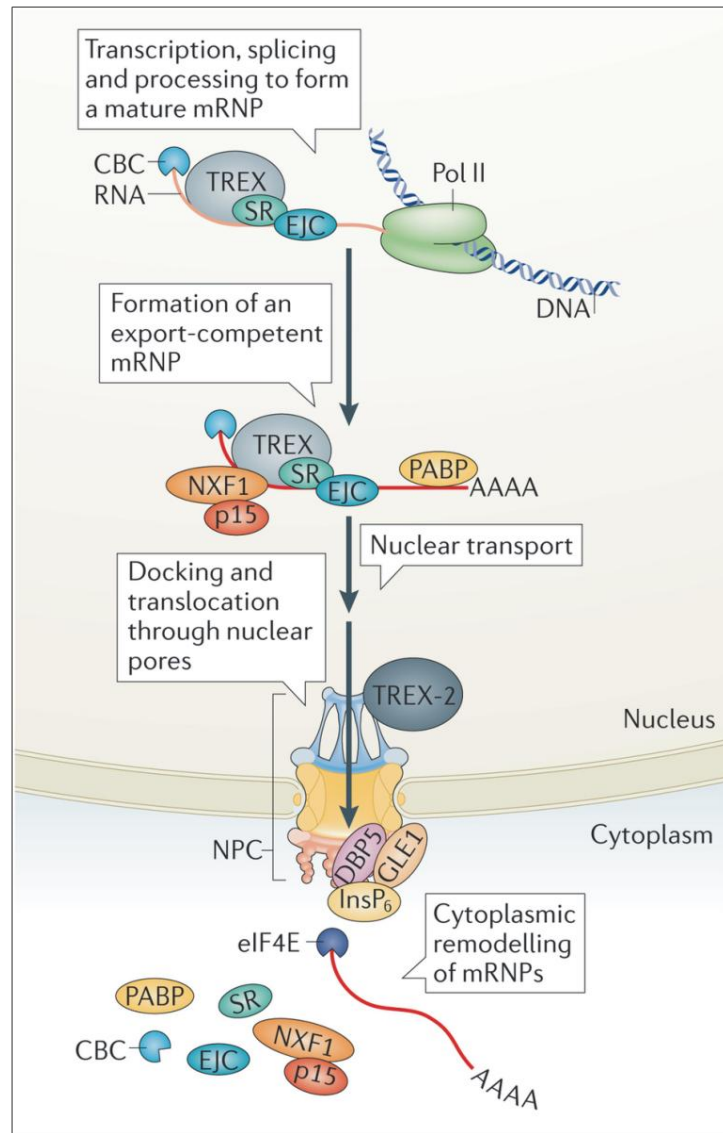


Fig 1.5 Diagram demonstrating the process of mRNA export from the nucleus. Firstly, a mature mRNP is formed by transcription, splicing and processing of the mRNA. Next the mRNP is conveyed to the Tap-p15 transport receptor (otherwise known as NXF1-p15) which, together with the TREX-2 complex, facilitates export of the mRNP through the NPC. Translation of the mRNA can then occur in the cytoplasm. Image Citation: Wickramasinghe, V. O., et al. (2015). "Control of mammalian gene expression by selective mRNA export." *Nat Rev Mol Cell Biol* **16(7)**: 431-442.

Image reproduced with the permission of Nature Publishing Group.

In response to DNA damage, the TREX complex can selectively enhance the export of mRNAs coding for specific DDR genes. For example, Aly is thought to be necessary for co-ordinating the export of mRNA coding for Rad51, Chk1 and FANCD2 (Wickramasinghe et al, 2013). The selective export of particular mRNAs following DNA damage allows continued expression of the required DDR genes whilst maintaining the global decline in expression of non-essential genes.

RBPs can prevent the formation of R-loops, and assist in their removal from the genome:

Aside from modifying DDR gene expression, certain RBPs, such as the THO components of the TREX complex, can prevent genomic instability by inhibiting R-loop formation. Null mutation of THO proteins in both yeast and humans has been shown to result in impaired transcription elongation, inhibited mRNA export, and increased genomic instability, in the form of DNA breaks and hyper-recombination (Dominguez-Sanchez et al, 2011; Jimeno et al, 2002). A chief cause of the inhibited transcription and hyper-recombination observed in THO mutants was revealed to be the accumulation of R-loops behind RNA Pol II. THO complex proteins are believed to prevent R-loop formation by stopping nascent mRNA from hybridizing with DNA during transcription. (Huertas & Aguilera, 2003). The TREX-2 complex has also recently been shown to be involved in preventing R-loop formation and consequent genomic instability, through its interaction with the HR repair protein BRCA2. (Bhatia et al, 2014).

The prevention of R-loop formation is not a role exclusive to RBPs responsible for mRNA export however. Proteins of the Fanconi anaemia (FA) pathway have been shown to be essential for the resolution of R-loops. The FA pathway currently consists of 18 genes, and homozygous inactivation of any of these leads to the Fanconi anaemia syndrome, which is characterised by chromosomal instability, bone marrow failure, and increased cancer predisposition. The FA genes can be subdivided into three subcomplexes and the largest of these, the core complex, consisting of FANCA, FANCB, FANCC, FANCE, FANCF, FANCG, FANCL and FANCM, has a critical role in activating the FA pathway through the monoubiquitination of the FANCD2 and FANCI proteins. These proteins then activate downstream Fanconi proteins, such as BRCA1, BRCA2, RAD51C and XPF, which are fundamental for DNA repair (Kee & D'Andrea, 2012; Wang, 2007).

Schwab et al. showed that knockdown of multiple FA gene products, such as FANCA, FANCL, and FANCD2 resulted in significantly increased formation of DNA: RNA hybrids (Schwab et al,

2015) Incubation of FANCD2 $-/-$ cells with RNase H1, an RBP which eliminates DNA: RNA hybrids by degrading the 3' end of the RNA strand, reduced R-loop formation. The FANCM protein, which possesses dsDNA translocase activity, was proposed as an enzyme potentially involved in resolving R-loops. FANCM was shown to unwind DNA: RNA hybrids in vitro, and biochemical analyses revealed that the protein can translocate along DNA strands in the 3' to 5' direction, and disrupt base-pairing between DNA and RNA. The findings of Schwab et al's study implicate FA pathway proteins, particularly FANCM, in the resolution of replication stress caused by R-loops.

Direct roles for RBPs in the DDR:

Finally, more than simply modulating the DDR, several RBPs have been shown to have direct roles within the DDR network. Recently, a proteomic screen identified the ubiquitin ligase PRP19, which is a key regulator of mRNA splicing, as a protein interacting with RPA-coated ssDNA (Maréchal et al, 2014). ssDNA can be exposed in a variety of situations, such as replication fork stalling, and during certain DNA repair pathways such as HR. The ssDNA is rapidly coated by Replication protein A (RPA), which acts as a platform for the recruitment of ATR, and its regulatory partner ATRIP, to the site of the damage. The activation of ATR on RPA coated ssDNA initiates cell cycle checkpoints, promotes DNA damage repair, and helps stabilize stalled replication forks (Cimprich & Cortez, 2008). PRP19 was found to localize to sites of RPA-coated ssDNA within cells, whereupon it promotes ubiquitylation of RPA, activates ATR, and encourages accumulation of ATRIP. Depletion of PRP19 resulted in decreased phosphorylation of both RPA and Chk1. Additionally, PRP19 knockdown cells exhibited defective recovery from replication fork arrest. These findings demonstrate that PRP19 has two distinct roles: in RNA processing, as a regulator of mRNA splicing, and in the DDR, where it senses RPA-ssDNA, activates ATR, and assists in replication fork restart.

A second example of direct involvement of RBPs in the DDR can be seen in the heterogeneous nuclear ribonucleoprotein U-like (hnRNPUL) proteins 1 and 2, which are involved in mRNA splicing (Bennett et al, 1992). Both of these proteins were shown to be recruited to DNA damage by the DSB-sensing MRN complex (Polo et al, 2012). Depletion of the proteins resulted in significantly impaired phosphorylation of Chk1, the secondary kinase targeted by ATR, suggesting impairment of ATR-dependent signalling. Since activation of ATR in response to DSBs relies upon the production of ssDNA by DNA end resection (Paques &

Haber, 1999), it was theorized that hnRNPUL 1 and 2 may be involved in 5'-3' resection of DSB ends prior to HR. Concurrent with this, depletion of the hnRNPUL 1 and 2 proteins was shown to significantly impair recruitment of the Bloom syndrome helicase (BLM), which is vital to 5'-3' resection (Sturzenegger et al, 2014). These findings indicate that hnRNPUL 1 and 2 are recruited to sites of DSBs by MRN, whereupon they activate the BLM helicase, thus promoting DNA end resection, and assisting in HR.

The idea of a functional interplay between RNA processing and the DDR is newly established, with much future research necessary to fully understand the interactions between the two. However, it has thus far, it has been recognized that RBPs can modulate DDR gene expression, prevent and resolve R-loop formation, and even function directly in the DDR, indicating RNA processing plays a significant and imperative role in maintaining genomic integrity.

1.4 CIP29

Human Cytokine induced protein 29, (CIP29) was first identified as a 24kDa novel nuclear protein over-expressed in liver and pancreatic tumours, and was designated Hepatocellular carcinoma 1 (Hcc-1). Fukuda et al, in their study to detect cytokine induced proteins in haematopoietic cells, identified a protein in the lysates of Erythropoietin (Epo)-stimulated leukaemic cells which possessed an identical genetic sequence to Hcc-1, which they then re-named CIP29. Sequence alignment has revealed that CIP29 has a yeast homologue, Tho1 (Jimeno et al, 2006b). Since its discovery, various properties of CIP29 have been described, and several, sometimes conflicting functions for the protein have been suggested. However, its exact purpose within the cell remains elusive.

Since its initial detection as a protein over-expressed in hepatocellular tumours, CIP29 expression has been shown to be increased in many other solid organ and haematological malignancies, and also in fetal tissues (Fukuda et al, 2002). The finding that CIP29 expression is enhanced in tissues with increased rates of proliferation, led to the idea that the protein may play a role in cellular proliferation, or in cell cycle control. Investigation into the potential involvement of CIP29 in cellular proliferation has yielded somewhat conflicting results. Fukuda et al. found that CIP29 mRNA expression seemed to correspond with the degree of cellular proliferation occurring in haematological cells. For example, when CD34+ cells were incubated with a growth factor cocktail known to maximally stimulate early stem and progenitor cell proliferation, increased expression of CIP29 mRNA was observed.

Similarly, erythropoietin-dependent UT7 cells starved of Epo demonstrated a progressive loss of CIP29 mRNA expression, with subsequent replacement of Epo resulting in up-regulated CIP29 mRNA expression. A greater proportion of Epo cultured cells progressed to the S or G2/M stages of the cell cycle. Conversely, Epo starved cells underwent progressive exit from the cell cycle, which appeared to correlate with the decline in CIP29 mRNA expression. Fukuda et al. concluded that CIP29 may play a role in regulating cell cycle progression, and as a result may influence cellular proliferation (Fukuda et al, 2002).

However, Leaw et al. reported that over-expression of CIP29 in HEK293 cells resulted in a slower growth rate in these cells compared to controls, and also led to an accumulation of cells at the G2/M cell cycle phase (Leaw et al, 2004). These studies suggest that CIP29 may play some sort of functional role in regulating cell cycle progression, but the exact nature of this role remains to be determined.

A second potential role for CIP29 is as an RBP involved in mRNA export. CIP29 has been shown to predominantly localize to the nucleus (Fukuda et al, 2002), and to possess a SAP motif, a putative eukaryotic DNA-binding module common to various proteins involved in DNA replication, transcription and regulation of DNA structure (Aravind & Koonin, 2000). This SAP domain is conserved in Tho1 (Jacobsen et al, 2016). CIP29 has been shown to bind to single and double-stranded DNA in vitro (Leaw et al, 2004), and also to RNA (Sugiura et al, 2007). These properties of CIP29, particularly its ability to directly bind to RNA, led to the idea that it is an RBP with a role in some aspect of RNA processing.

Several studies have suggested that CIP29 may be involved in mRNA export. The yeast homologue of CIP29, Tho1, was first identified as a multicopy suppressor of various THO complex mutant phenotypes, including RNA export defects, increased R-loop formation and the associated hyperrecombination (Jimeno et al, 2006a). Somewhat incongruously, recruitment of Tho1 to nascent mRNA was shown to be dependent on the presence of the THO complex. Jimeno et al. proposed a model in which the THO complex ordinarily facilitates the loading of Tho1, and the Aly homologue Sub2, onto nascent mRNA, where they assist in the formation of an mRNP ready nuclear for export. When overexpressed in THO mutants, Tho1 somehow circumvents the need for the THO complex and can bind to mRNA regardless, perhaps because overexpression increases the probability of the protein binding to mRNA. Tho1 then facilitates mRNP biogenesis even in the absence of the THO complex. This study suggests a vital role for Tho1 in orchestrating an alternative mRNA export pathway triggered by absence of the THO complex. However, despite the functional

relationship between Tho1 and the mRNA export machinery, no mRNA export defect could be detected in Tho1 mutants, nor did they display the R-loop associated genomic instability seen in the THO complex mutants.

Dufu et al. investigated the possible involvement of CIP29 in mRNA export (Dufu et al, 2010). An mRNA export defect could not be detected following siRNA knockdown of CIP29, possibly due to functional redundancy, but over-expression of CIP29 did inhibit mRNA export, indicating some involvement in this process. CIP29 was found to possess the same subcellular localization patterns as components of the TREX complex, and was able to co-immunoprecipitate with all known TREX proteins. Furthermore, like TREX complex components, CIP29 was shown to be recruited to mRNA in a splicing and cap-dependent manner. This led to the suggestion that CIP29 may be a newly identified conserved component of the TREX complex.

Immunodepletion experiments exploring specific interactions between CIP29 and TREX components, revealed that CIP29 forms a ATP-dependent trimeric complex with UAP56 and Aly (Dufu et al, 2010). UAP56 is a member of the DEAD-box RNA helicase family, which is involved in the unwinding of dsRNA (de la Cruz et al, 1999), and it is thought that Aly may be involved in stimulating the helicase activity of UAP56 (Chi et al, 2013). The CIP29/UAP56/Aly complex was shown to be recruited to the 5' end of mRNA and it was therefore proposed that it could be involved in unwinding the 5' end of the mRNA, thus allowing recruitment of the THO complex, and/or efficient transmission of the mRNP through a nuclear pore complex. Dynamic changes in the interactions between CIP29, UAP56 and Aly were observed when the levels of ATP were altered. In the presence of ATP, the three proteins co-immunoprecipitated with each other, and with the THO complex. Contrastingly, in the absence of ATP, UAP56 co-immunoprecipitated with the THO complex, but not with either CIP29, or Aly. This led to the suggestion that the CIP29/UAP56/Aly complex may be involved in remodelling the TREX complex, and thus regulating mRNA export.

Yamazaki et al. examined the functions and interactions of UAP56 and its homolog URH49 in human cells, and revealed possible involvement of CIP29 in both mRNA export and mitotic progression (Yamazaki et al, 2010). SiRNA knockdown of UAP56 and URH49 inhibited nuclear export of mRNA, and also led to defects in mitotic progression. An increased frequency of chromosome misalignment was found in the UAP56i and URH49i cells, a phenomenon known to activate the spindle assembly checkpoint (SAC), which is involved in co-ordinating mitotic arrest. The proportion of UAP56i and URH49i cells in each mitotic phase was then

quantified, revealing that knockdown of both proteins does indeed lead to mitotic delay during prometaphase. On mitotic chromosome spreads, distinct mitotic defects were observed: premature sister chromatid separation (PMSCS) was seen in the UAP56i cells, whereas in URH49i cells, chromosome arm resolution defects were seen. Knockdown of both UAP56 and URH49 was shown to down-regulate expression of specific genes necessary for mitotic progression, which correlated with the mitotic progression defects seen in each.

Immunoprecipitation experiments to identify related factors revealed that while UAP56 preferentially associates with the THO complex and Aly, URH49 associates with CIP29. It was proposed that UAP56 binds the THO complex and Aly to form the TREX complex, whereas URH49 and CIP29 combine to form an alternative mRNA export (AREX) complex. Contrary to Dufu et al.'s finding, knockdown of CIP29 did result in an mRNA export defect, as did knockdown of the THO complex, and Aly. However, while the THOi and Alyi cells did demonstrate mitotic delay with chromosome misalignment, the CIP29i cells did not exhibit significant mitotic delay. Like the UAP56i cells, the THOi and Alyi cells exhibited PMSCS on chromosome spreading, whereas CIP29i cells demonstrated chromosome arm resolution defects similar to those seen in URH49i cells. These findings led to the conclusion that CIP29, as part of the AREX complex, plays a role in mRNA export, and may also be involved in chromosome arm resolution.

Previous laboratory research into CIP29:

Previous research into CIP29 carried out by this laboratory has focused upon the characterisation of *X.laevis* CIP29 (XCip29), which shares a high degree of homology (72% identical sequence) with the human CIP29 protein (Holden, 2014).

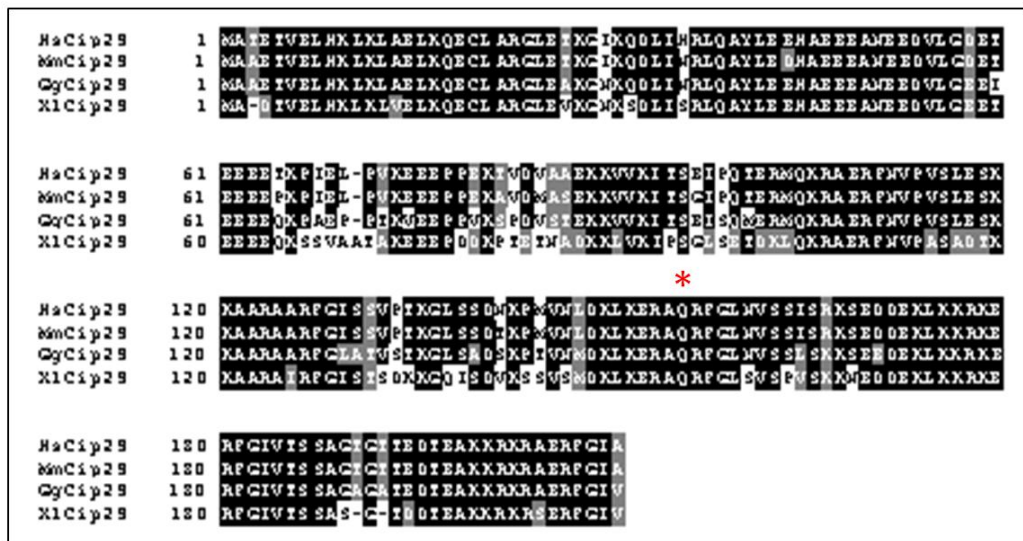


Fig 1.6 Diagram demonstrating the sequence alignment of CIP29 in humans, mice, chickens, and frogs.

XCip29 was shown to be phosphorylated in response to DNA damage in the form of dsDNA ends. (Fig 1.7).

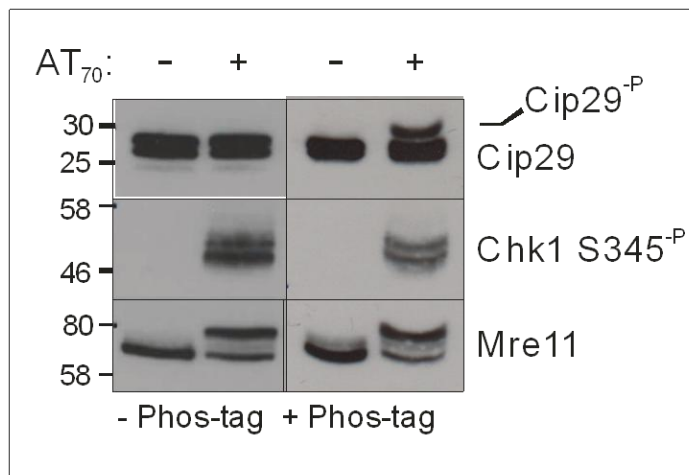


Fig 1.7 Phosphorylation of XCip29 in *Xenopus* egg extract in the presence of linear dsDNA. These Western blots demonstrate a phosphorylation shift of XCip29 in response to treatment of *Xenopus* extract with AT70, which is known to mimic DSB damage. Phosphorylation of Chk1 and Mre11 confirms that a checkpoint response has been induced by AT70. Image Citation: Holden, J. (2014). Characterisation of Cip29: A novel target of the eukaryotic DNA damage response B.Sc. (Hons), Lancaster University.

This damage-dependent XCip29 phosphorylation was shown to be dependent upon the activity of the PI3KK kinase ATM (Fig 1.7). As previously mentioned, ATM is mainly activated in response to DSBs, but is also involved in the DDR to oxidative damage and R-loops.

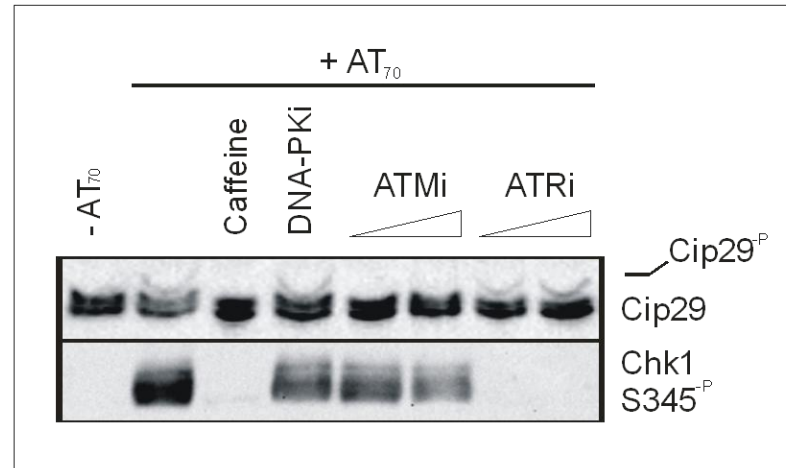


Fig 1.8 Phosphorylation of XCip29 is dependent upon ATM activity. Phosphorylation of XCip29 is shown to be abolished following treatment with caffeine, a global inhibitor of the PI3KK kinases. When *Xenopus* extract was incubated with a specific ATM inhibitor, this abolished XCip29 phosphorylation, but treatment with DNA-Pk and ATR inhibitors did not. This indicates that XCip29 phosphorylation is dependent upon ATM activity. **Image Citation:** Holden, J. (2014). Characterisation of Cip29: A novel target of the eukaryotic DNA damage response B.Sc. (Hons), Lancaster University .

The XCip29 amino acid sequence was analysed to detect potential damage-dependent phosphorylation sites. Typically, ATM preferentially phosphorylates substrates on serine or threonine residues preceding glutamine residues, so called S/T-Q or consensus sites (Kim et al, 1999). However, perhaps surprisingly, no S/T-Q consensus sites were identified on XCip29. The residue Ser95, which lies within a consensus recognition motif for the protein kinase Chk1, was identified as the major DNA damage-dependent phosphorylation site on XCip29. This site (indicated with a star in Fig 1.6), is conserved in human CIP29. Since XCip29 phosphorylation was found to be ATM-dependent, the fact that the major damage-dependent phosphorylation site on XCip29 is not an S/T-Q site is unusual. It was proposed that XCip29 may not be phosphorylated directly by ATM, but by protein kinases downstream of ATM signalling, such as Chk1 or Chk2. However, immunodepletion of both of these proteins did not impact on XCip29 phosphorylation.

There are a number of possible explanations for these findings. There are examples of ATM-dependent protein phosphorylation occurring on non-consensus sites. For example, the transcription factor p53, which plays an important role in apoptosis, is degraded by Mdm2.

ATM phosphorylates p53 in the Mdm2-interacting N-terminal region, at the non-consensus site Ser15, and in doing so also stabilizes p53 by weakening its interaction with Mdm2 (Banin et al, 1998). An additional example is the centrosomal protein Cep63 which is involved in normal spindle assembly. *Xenopus* Cep63 is phosphorylated by ATM on Ser560, which is also not an S/T-Q site (Smith et al, 2009). ATM could therefore be responsible for phosphorylation of XCip29, on a non-S/T-Q site.

Additionally, Holden's observations were based on in-vitro kinase assays, and there are examples of proteins being phosphorylated differently in vivo compared to in vitro. For example, Gardiner et al. found FUS to be a target of DNA-PK in vitro, whereas in vivo, FUS phosphorylation was not affected by DNA-PK inhibition but was significantly reduced by inhibition of ATM (Gardiner et al, 2008). Therefore, a second possibility is that XCip29 is not actually phosphorylated by ATM in vivo.

Bensimon et al. recently reported that, following radiomimetic treatment of human melanoma cells, only a relatively small proportion of the DSB-induced phosphorylation events occurred on S/T-Q sites. 40% of the phosphorylation events appeared to occur independently of ATM. These findings suggest the involvement of multiple other kinases in the DDR to DSBs, aside from ATM, so XCip29 could conceivably be a target of one of them. (Bensimon et al, 2010).

1.5 This Thesis

This introduction has outlined the workings of the DDR, including the DDR response to DSBs, the importance of the PI3KK kinase ATM, and the recent research into the involvement of RNA-binding proteins in the DDR. The limited scientific literature focusing on the protein CIP29 has also been described. Several potential roles for CIP29 have been suggested, including as an RNA-binding protein implicated in mRNA export, in the regulation of cellular proliferation, and carcinogenesis. However, the exact role of this protein remains unclear. Previous research by this laboratory has identified CIP29 as a DNA-damage dependent target of ATM in *X.laevis* egg extracts.

Given the high degree of conservation in the DDR signalling pathways of eukaryotes, and considering the complex interplay between RNA processing and the DDR that has now been recognised, we considered it probable that CIP29 is also a DDR target in human cells.

Therefore, the work presented in this thesis has built upon the findings of the previous laboratory research, by extending the studies into human cells. We attempted to ascertain whether the human CIP29 protein is phosphorylated in response to DNA DSBs, and explored whether XCip29 phosphorylation in human cells is dependent upon PI3KK kinase activity, as it is in *Xenopus* extract. Furthermore, CRISPR genome editing was used to generate two CIP29 knockout cell lines, which were then characterised. Experiments were carried out to assess the impact of CIP29 knockout on cellular proliferation, cell cycle progression and mitotic progression, and thus ascertain whether CIP29 is likely to play a role in these cellular processes. Additionally, sensitivity of the knockout cells to several DNA damaging agents was investigated, with the aim of determining whether CIP29 is involved in the DDR in human cells.

Chapter 2: Materials and Methods

Table 2.1 Composition of buffers and solutions used in this work.

Solution:	Composition:
Buffer TE	10mM Tris pH 8, 1mM EDTA
1 x TBE	0.1M Tris-base, 0.1M Boric acid, 0.002M EDTA
6 X loading buffer for agarose gel electrophoresis	30% glycerol, 0.25% bromophenol blue, 0.25% xylene cyanol FF
MP1	50mM glucose, 25mM Tris pH8, 10mM EDTA
MP2	200mM NaOH, 1% SDS
MP3	3M KOAc, 2M HOAc
Genomic DNA lysis buffer	100mM Tris, 5mM EDTA, 200mM NaCl, 0.2% SDS, 0.1mg/ml proteinase K
Wash buffer for total cell extracts	50mM Tris pH 7.5, 150mM NaCl 1mM MgCl ₂
Lysis buffer for total cell extracts	50mM Tris pH 7.5, 150mM NaCl, 1mM MgCl ₂ , 0.1% SDS, 1µl/ml Base muncher (Expedeon), Protease Inhibitor Cocktail (Sigma-Aldrich®) at 1/100. For preservation of protein phosphorylation, the following was added: 10mM NaF, 10mM β-glycerophosphate 2mM Na ₂ VO ₃ .
5 X loading buffer for SDS-PAGE electrophoresis	0.25% bromophenol blue 0.5M dithiothreitol, 50% glycerol, 10% SDS
SDS-PAGE running buffer	24.8mM Tris-base, 192mM, 0.1% SDS
Transfer buffer (for wet and semi-dry transfer)	48mM Tris-base, 39mM Glycine, 20% methanol
PBS	50mM potassium phosphate, 150mM NaCl, pH 7.2
PBS-T	PBS plus 0.1% Tween
ECL reagent	20ml of 100mM Tris pH 8.0 with 6µl of hydrogen peroxide (30% solution), 50µl of 90mM p-coumaric acid and 100µl of 250mM luminol.
Mild stripping buffer	200mM glycine pH2, 0.1% SDS
Harsh stripping buffer	62.5mM Tris PH 6.8, 2% SDS, 100mM β-mercaptoethanol
Methylene blue stain	50% methanol, 0.5% methylene blue
Fix solution	3:1 ratio of methanol to glacial acetic acid
Growth medium	DMEM medium containing 10% fetal bovine serum and 1% penicillin/streptomycin

2.1: Molecular Biology Techniques

2.1.1: Restriction digests

Preparative-scale restriction digests were routinely prepared in a total volume of 40 μ l, containing 10 μ g DNA and 10-20 units of the appropriate restriction enzyme(s) and restriction enzyme buffer (NEB[®]).

Diagnostic restriction digests were set up using approximately 1 μ g DNA in a 20 μ l total volume, containing 3-6 units of the appropriate restriction enzyme(s) and restriction enzyme buffer.

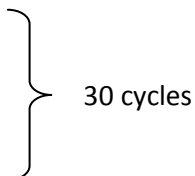
All digests were incubated at 37°C for 1-3h.

2.1.2: Polymerase Chain Reaction (PCR)

For PCR amplification, 25 μ l PCR reactions were set up containing 5 μ l 5x Q5 buffer, 2 μ l 2.5mM dNTPs, 0.25 μ l of each primer, 0.25 μ l Q5 polymerase (NEB) and approximately 5ng plasmid or 100ng genomic template DNA. For negative controls, water was used instead of DNA. The PCR reactions then underwent thermal cycling using settings optimized for each PCR template. For PCR performed on the XCip29 template, thermal cycling settings were as follows:

98°C- 30s

98°C-10s
55°C-30s
72°C-30s



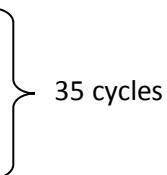
30 cycles

72°C-2 min.

For PCR performed on the CIP29 template from MRC5, C9 and C60 genomic DNA, thermal cycling settings were as follows:

98°C-30s

98°C-10s
60°C-20s
72°C-30s



35 cycles

72°C-2 min.

Table 2.2 PCR primers:

Primer:	Sequence:	Use:
EP41	5'-CTA AGA TGT AGG TTG TAC AAG ATG GC-3'	PCR of CIP29 template from MRC5, C9 and C60 genomic DNA.
EP42	5'-GGA TCT GGG ATA ATA AGT GGT AAG G-3'	PCR of CIP29 template from MRC5, C9 and C60 genomic DNA.
EP49	5'-ACT CGA GAT GGC GGA CAC AGT GGA GCT TCA C-3'	PCR of XCip29 template
EP50	5'-AGT CGA CCT AGA CAA TGC CAA AGC GTT C-3'	PCR of XCip29 template

2.1.3: Purification of PCR products using the QIAquick® PCR Purification Kit

DNA fragments generated through PCR amplification and restriction digestion were purified using the QIAquick (QIAGEN®) PCR purification kit, according to the manufacturer instructions.

2.1.4: Ethanol precipitation of PCR products

Where desired, ethanol precipitation was performed to increase the concentration of purified PCR products. A 1/10 volume of 3M Sodium acetate and 3 volumes of 100% ethanol were added to the purified PCR product and the mixture centrifuged (13,000rpm, 10 min). The supernatant was removed and the DNA pellet air-dried for 2 min. The pellet was resuspended in Buffer TE (10mM Tris pH 8, 1mM EDTA).

2.1.5: A-tailing of PCR products

To a-tail blunt ended PCR products, 10µl total mixtures were made up containing approximately 1µg purified PCR product, 1µl TAQ buffer, 1µl TAQ polymerase (NEB®) and 1µl 2mM dATP. The reactions were heated at 70°C for 2 min.

2.1.6: Gel Electrophoresis

For agarose gel electrophoresis of DNA, gels were made with 0.8g agarose in 100ml 1 x TBE (0.1M Tris-base, 0.1M Boric acid, 0.002M EDTA), placed in the electrophoresis apparatus, and submerged in 1 x TBE. DNA samples, combined with 6 x loading buffer (30% glycerol, 0.25% bromophenol blue, 0.25% xylene cyanol FF) were loaded and gels were run at 100V for 45 min. Gels were stained for 30 min in 50ml 1xTBE containing 15µl Gelred® stain, and then visualized on a UV transilluminator.

2.1.7: QIAquick Gel Extraction

The desired DNA fragment was excised from the gel under UV light, using a scalpel. The fragment was weighed, and processed according to the recommended QIAquick® Gel Extraction Kit protocol (QIAGEN®).

2.1.8: Ligation

Ligations into the PCI-Flag vector were set up with a 3:1 ratio of DNA fragment to plasmid vector. 10µl ligation mixtures, containing 5µl 2x quick ligase buffer (NEB®), 0.5µl PCI-Flag vector, 4µl a-tailed PCR product, and 0.5µl of T4 DNA Ligase (Invitrogen™) were incubated at room temperature for 1h.

Ligations into the pGEM®-T Easy vector were carried out in a total volume of 10µl, with 5µl 2x rapid ligation buffer, 0.5µl of pGEM®-T Easy vector (Promega®), 4µl a-tailed PCR product, and 0.5µl T4 DNA ligase (Promega®). The ligation reaction was incubated at room temperature overnight.

2.1.9: Transformation of plasmids into chemically competent E.coli DH5a cells

5µl of ligated DNA was added to 50µl DH5a cells, and the combination mixed gently. The cells were incubated on ice for 30 min, heat-shocked at 42°C for 45s and then incubated on ice for 2 min. 800µl of LB medium was added and the cells were incubated at 37°C for 1h. Following incubation, the cells were spun (13,000rpm, 30s) and 700µl medium was removed. Cells were resuspended in the residual 100µl, plated on a selective agar plate containing 100µg/ml ampicillin and incubated overnight at 37°C.

2.1.10: Alkaline lysis miniprep method

For small-scale plasmid DNA preparation prior to restriction digest screening, colonies from selective agar plates were inoculated into 2ml of LB medium plus carbenecillin (100mg/ml) and grown at 37°C overnight, or until cloudy. Cells were harvested from 1.5ml culture (13,000rpm, 30s) and the cell pellet resuspended in 100µl of MP1 (50mM glucose, 25mM Tris pH8, 10mM EDTA). 200µl of MP2 (200mM NaOH, 1% SDS) was added, followed by 150µl of MP3 (3M KOAc, 2M HOAc). After mixing, the samples were spun (13,000rpm, 30s) and the supernatant transferred to a new microcentrifuge tube. 1ml of 100% ethanol was added, the solution was mixed and spun (13,000rpm, 10min) and the cell pellet resuspended in 30-50µl of water.

2.1.11: QIAGEN® Miniprep method

For small-scale plasmid DNA preparation prior to sequencing, colonies from selective agar plates were inoculated in 2ml of LB medium plus carbenecillin (100mg/ml) and grown at

37°C overnight, or until cloudy. Cells were then harvested by centrifugation (5000rpm, 10 min). Plasmid DNA was then prepared using the QIAGEN® Miniprep kit, according to the manufacturer's instructions.

2.1.12: QIAGEN® Midiprep method

For large-scale plasmid DNA preparation, cells from 100ml bacterial culture were harvested by centrifugation (5000rpm per g, 15 min, 4°C). The pellet was resuspended in 4ml of Buffer P1 (containing RNase) and mixed to ensure complete suspension. 4ml of Buffer P2 and Buffer P3 were added sequentially, with mixing, before centrifugation (5000rpm per g, 15 min, 4°C). The supernatant was collected and the DNA precipitated by the addition of 10ml isopropanol followed by centrifugation (5000rpm, 15 min, 4°C). The DNA pellet was resuspended in 500µl of TE buffer, and 4.5ml of buffer QBT was added. This solution was applied to a QIAGEN®-tip, equilibrated with QBT buffer, or, if the midiprep was to be used for transfection, 10% Triton X-100 was added to the DNA solution and the mixture incubated at 4°C for 30 min before application to the equilibrated QIAGEN®-tip. In each case, the QIAGEN®-tip was washed twice with 10ml Buffer QC, before the DNA was eluted with 5ml Buffer QF. Finally, the eluted DNA was precipitated by the addition of 3.5ml isopropanol and centrifugation (5000rpm, 30min, 4°C). The DNA pellet was washed with 5ml of 70% ethanol, air-dried for 5-10 min, and redissolved in 0.4ml of Buffer TE.

2.1.13: Preparation of genomic DNA

Cell pellets (approximately 2×10^6 cells) were resuspended in 300µl of lysis buffer (100mM Tris, 5mM EDTA, 200mM NaCl, 0.2% SDS, 0.1mg/ml proteinase K), and incubated at 37°C for 1h. An equal volume of phenol was added and mixed gently to emulsify. The mixture was centrifuged (13,000rpm, 4min) and the aqueous phase transferred to a new microcentrifuge tube using a cut pipette tip, to prevent shearing of the DNA. To remove all traces of phenol, this process was repeated with equal volumes of phenol-chloroform and chloroform. Genomic DNA was precipitated by the addition of two volumes of isopropanol and incubation at -20°C overnight. The DNA was then pelleted by centrifugation (13,000rpm, 10 min), the pellet washed with 500µl of 70% ethanol, and briefly air dried before resuspension in an appropriate volume of Buffer TE.

2.2: Protein Methods:

2.2.1: Preparation of total cell extracts

Harvested cell pellets or adherent cells *in situ* were washed with 0.5ml wash buffer (50mM Tris pH 7.5, 150mM NaCl 1mM MgCl₂), then resuspended in 40-100µl of lysis buffer (50mM

Tris pH 7.5, 150mM NaCl, 1mM MgCl₂, 0.1% SDS, 1μl/ml Base muncher (Expedeon), Protease Inhibitor Cocktail (Sigma-Aldrich®) at 1/100. Where preservation of protein phosphorylation was desired, phosphatase inhibitors were included in the lysis buffer as follows: 10mM NaF, 10mM β-glycerophosphate 2mM Na₂VO₃. Cells were lysed at room temperature for 10 min, and the extract was clarified by centrifugation (13,000rpm, 4 min, 4°C).

2.2.2: Bradford assay method

Bradford assays were performed to determine protein concentration. 10μl of protein solution/cell extract was mixed with 1ml Protein Assay Dye Reagent (Bio-rad) in a cuvette, and the colour change, relative to 'buffer only' control, was measured on a spectrophotometer at OD600.

2.2.3: SDS-PAGE Electrophoresis

Biometra gel electrophoresis apparatus was routinely used for SDS-PAGE. The gel plates were assembled and the resolving gel, prepared according to Table 2.1, was poured into the gel plates, and overlaid with water saturated butan-2-ol to remove any air bubbles. After the gel was set (approximately 40 min) the excess butan-2-ol solution was poured off ,the stacking gel (Table 2.2) poured in, and the combs inserted. This was allowed to set for 15-20 min.

Table 2.3 Recipes for 10ml of resolving gel for SDS-PAGE.

Component	8% gel Volumes (ml)	10% gel Volumes (ml)	12% gel Volumes (ml)	14% gel Volumes (ml)
ddH ₂ O	4.6	4.0	3.3	2.6
30% acrylamide mix	2.7	3.3	4.0	4.7
1.5M Tris (pH 8.8)	2.5	2.5	2.5	2.5
10% SDS	0.1	0.1	0.1	0.1
10% APS	0.1	0.1	0.1	0.1
TEMED	0.006	0.004	0.004	0.004

Table 2.4 Recipe for 3ml of stacking gel for SDS-PAGE.

Component	Volume (ml)
ddH ₂ O	2.1
30% acrylamide mix	0.5
1.0M Tris (pH 6.8)	0.38
10% SDS	0.03
10% APS	0.03
TEMED	0.003

Cell extracts were combined with 5 x loading buffer (0.25% bromophenol blue 0.5M dithiothreitol, 50% glycerol, 10% SDS) and loaded onto the gel. Electrophoresis was run through 1 x SDS-PAGE running buffer (24.8mM Tris-base, 192mM glycine, 0.1% SDS) at a constant voltage of 120V through the stacking gel, and 160V through the resolving gel, until the blue dye front ran off (approximately 90 min.)

Phos-Tag™ SDS-PAGE Electrophoresis:

For increased resolution of phosphorylated proteins, Phos-Tag™ ligand gels were prepared, as per the recipe below. Stacking gels were made up as per Table 2.2. Electrophoresis was performed through 1 x SDS-PAGE running buffer, at a constant current of 30mA, until the blue dye front ran off (approximately 70 min.) Gels were soaked, with gentle agitation, in 50ml of 1 x transfer buffer (48mM Tris-base, 39mM Glycine, 20% methanol) with 10mM EDTA, for 2 x 10 min, then for 10 min in transfer buffer without EDTA, before Western transfer.

Table 2.5 Recipe for 6ml of Phos-Tag™, 8% w/v acrylamide resolving gel.

Component	Volume (ml)
ddH ₂ O	2.7
30% bis-acrylamide	1.6
1.5M Tris pH 8.8	1.5
10% SDS	0.06
5mM Phos-Tag™	0.024
10mM MnCl ₂	0.018
10% APS	0.085
TEMED	0.017

2.2.4: Western blotting

Semi-dry transfer:

Used for the transfer of proteins from standard SDS-PAGE gels:

Three pieces of filter paper and a nitrocellulose membrane were soaked in transfer buffer. A Western transfer sandwich was assembled in the semi-dry transfer apparatus (Bio-rad) as follows: Filter paper x2, nitrocellulose membrane, gel, filter paper. Any air bubbles between the layers were rolled out during the assembly of the sandwich. Proteins were transferred at 15-20 V for 1h.

Wet transfer:

Used for the transfer of proteins from Phos-Tag™ SDS-PAGE gels:

Two pieces of filter paper, a nitrocellulose membrane, and the Phos-Tag™ SDS-PAGE gel were soaked in transfer buffer solution. They were then assembled as a sandwich in a gel holder cassette as follows (from bottom to top): Foam blotting pad, 1 piece of filter paper, Phos-Tag™ gel, nitrocellulose membrane, 1 piece of filter paper, foam blotting pad. Any air bubbles between the layers were rolled out during assembly. The cassette was then placed in a Mini-Trans-Blot® electrophoretic transfer cell, filled with transfer buffer, and proteins transferred at 100V, with continuous stirring of the buffer.

2.2.5: Staining the nitrocellulose membrane with antibody

Nitrocellulose membranes were incubated in milk blocking buffer (5% powdered milk in PBS-T (PBS plus 0.1% Tween)) for 1h at room temperature. Filters were then incubated in the chosen primary antibody (5% in milk) overnight at 4°C. The primary antibody was then poured off, and the filter was washed for 4x 5 min in PBS-T. The membrane was incubated with the appropriate HRP secondary antibody for 1h at room temperature, and again washed for 4x 5 minutes in PBS-T.

Table 2.6 The primary antibodies used in my experiments.

Antibody	Origin	Supplier	Concentration
CIP29	Rabbit	Raised in-house	1:1000
H2AX	Mouse	Upstate Biotechnology, Inc.	1:1000
GAPDH	Mouse	Abcam	1:1000
FLAG	Mouse	Sigma-Aldrich®	1:1000

2.2.6: Developing Western Blots by Enhanced Chemiluminescence (ECL)

After the secondary antibody had been washed off, the membrane was blotted dry. ECL reagent was prepared by mixing 20ml of 100mM Tris pH 8.0 with 6µl of hydrogen peroxide (30% solution), 50µl of 90mM p-coumaric acid, and 100µl of 250mM luminol. The reagent was poured onto the nitrocellulose membrane. After, 1 min, the filter was blotted dry, wrapped in clingfilm and imaged using the Chemi blot setting on the Bio-rad ChemiDoc™.

2.2.7: Stripping Western Blots

Under Mild Stripping Conditions: The nitrocellulose filter was washed for 2x 5 min in mild stripping buffer (200mM glycine pH2, 0.1% SDS) at room temperature. It was rinsed twice and then washed for 3x 5 min in PBS-T.

Under Harsh Stripping Conditions: The nitrocellulose filter was submerged in harsh stripping buffer (62.5mM Tris PH 6.8, 2% SDS, 100mM β -mercaptoethanol) at 50°C for 30 min, with occasional shaking. The filter was then rinsed twice and then washed for 3x 5 min in PBS-T.

After stripping, the nitrocellulose membranes could be blocked and re-probed with the desired antibodies.

2.3: Cell Culture Techniques

2.3.1. Cell culture conditions

MRC5-V1 cells and derivatives thereof were routinely grown in DMEM medium (Lonza) containing 10% fetal bovine serum (Hyclone™) and 1% penicillin/streptomycin (Gibco™) at 37°C in 5% CO₂.

For routine subculture, the medium was removed by aspiration and the cells were washed in PBS and then incubated in 5% trypsin solution (5% trypsin (Gibco™) in PBS). The trypsinized cell solution was spun down through an equal volume of medium, then the cell pellet was resuspended in growth medium, and the cell suspension used as required.

Cells were frozen in cryovials, at an approximate concentration of 1-2 x 10⁶/ml, in medium containing 10% DMSO. The cryovials were placed in a freezing vessel at -80°C overnight, then transferred to liquid nitrogen for long-term storage.

Once removed from liquid nitrogen storage, cells were quickly thawed by placing the cryovials in a 37°C waterbath. Once thawed, the cells were transferred into a centrifuge tube containing 5ml medium, and harvested at 500rpm for 5 min.

2.3.2. Plasmid Transfection

Cells grown to approximately 70% confluency on a 24- well plate were transfected using Turbofect transfection reagent (Thermo Fisher Scientific) as follows. For each reaction, 1 μ g of plasmid was diluted in 100 μ l of serum-free growth medium (Lonza). 2 μ l transfection reagent was added to the diluted DNA, and mixed by vortexing. After incubation at room temperature for 15-20min, 100 μ l of the transfection mixture was added drop-wise to each well and the plate was gently rocked to evenly distribute the complexes.

For transient transfections, cells were then incubated under normal growth conditions for 24h before analysis.

For isolation of stable transfectants, cells were incubated under normal growth conditions for 48h, then the transfected cells were trypsinised and re-plated between three 10cm

plates in medium containing 800µg/ml G418. After approximately 14 days, individual colonies were isolated. The medium was removed from each plate by aspiration and the colonies washed with PBS. Sterile tweezers were used to place filter paper circles soaked in trypsin solution over individual colonies, and the plates incubated at 37°C for 5 min. After trypsinisation, each paper cloning disc was transferred to an individual well of a 24-well plate containing 1ml medium with G418, and grown under normal conditions for several days prior to subculture of the stable transfectant cells.

2.3.3 Metabolic Proliferation assay

To determine the proliferation rate of various cell lines, the WST-1 Quick Cell Proliferation Assay Kit (Abcam) was used to monitor cell growth over a four day period. Routinely, 5×10^3 cells were plated in 100µl medium in triplicate, on five 96-well plates, and grown under normal conditions. At the start of the experiment, 10µl of WST-1 reagent was added to each 100µl of cell suspension on the 1st 96-well plate, and after incubation for 1h at 37°C, the concentration of formazan dye in each cell suspension was measured using a PerkinElmer® plate reader (450nm, 0.1s). At 24h intervals thereafter, the medium from a single 96-well plate was removed and replaced with 100µl of medium plus 10µl WST-1 reagent, and after incubation for 1h at 37°C, formazan dye concentration was measured as described. For each 96-well plate, a control measurement was made, in triplicate, using medium and WST-1 reagent alone.

2.3.4 Cytotoxicity Assay

To determine drug sensitivity, cells were placed at 1×10^4 cells per well on a 96-well plate, in 200µl medium, (three wells per drug dose) and incubated overnight under normal growth conditions. The following day, the medium was replaced with fresh medium containing different concentrations of a DNA damaging agent, in triplicate. For camptothecin (CPT) treatment, medium was supplemented with 0, 100, 500 or 1000nM CPT (2mM stock solution, Sigma-Aldrich). For etoposide treatment, medium was supplemented with 0, 5, 10 and 20 µM (from 50mM stock solution, Sigma-Aldrich). Cells were grown under normal conditions for 72h, then the medium was replaced with fresh 100µl of fresh medium, plus 10µl of WST-1 reagent. The plate was incubated at 37°C for 1h, before the formazan dye concentration was measured on a PerkinElmer® plate reader (450nm, 0.1s). A control measurement was made, in triplicate, using medium and WST-1 reagent alone.

2.3.5 Clonogenic survival assay

To assay cells for sensitivity to Neocarzinostatin (NCS), cells were grown to 70% confluency, before the addition of NCS to the growth medium to a final concentration of 0-15nM

(4.5Mm stock, Sigma-Aldrich) and incubation for 1h at 37°C. After drug treatment, the cells were harvested, counted and plated in duplicate at varying cell densities ranging from 500-100,000 cells/10cm plate. The plates were incubated at 37°C for 10 days, to allow colony formation. The medium in each plate was then carefully removed, and the colonies bathed in 0.5% methylene blue stain (50% methanol, 0.5% methylene blue) for 30 min. Plates were rinsed with water, and the number of colonies on each plate was counted. The amount of colony formation on each plate was used to determine the survival rates of cells treated with differing concentrations of NCS. The plating efficiency for each cell line was calculated by dividing the average number of colonies on the untreated plates, by the total number of cells plated. The survival fraction for each cell line and drug dose was calculated by dividing the number of colonies on the plate by the number of cells plated, and then multiplying that number by the plating efficiency for the cell line.

2.3.6 Chromosome spreading

Cells were grown to 80-90% confluency in a T25 flask, and colcemid (KaryoMAX®) was added to a final concentration of 10ng/ml for 2-6h. Then the cells were harvested, and the cell pellet resuspended in 5ml of pre-warmed 0.075M potassium chloride (KCl), added dropwise, with continuous agitation. Cells were incubated in KCl for 20 min at 37°C (timed from the start of KCl addition), then 5ml of fix solution (3:1 solution of methanol: glacial acetic acid) was added dropwise, on ice. The fixed cell solution was gently inverted and then spun (500rpm, 5 min). The supernatant was discarded, and the pellet resuspended in 8ml of fix solution, added in 0.5ml increments. This wash step was repeated four times. Finally, the cell pellet was resuspended in 200-1000µl of fix solution, depending on the cell density and solution translucency.

For chromosome spreading, each glass microscope slide was rinsed in fix solution and allowed to briefly air dry. The slide was breathed on, then 40µl of fixed cell suspension was immediately dropped on to it from a height of ~ 10cm. 5 drops of fix solution were pipetted on top and the slide was tilted gently ten times, before being stood up to drain. As the cells became visible, 2-3 further drops of fix were pipetted on top. The slide was left to dry, before staining, either with Giemsa™ for light microscopy or with DAPI mounting solution (Vectashield®) for fluorescent microscopy.

2.3.7 Fluorescent Advanced Cell Sorting (FACS)

For FACS analysis, cells grown to medium confluency were harvested, and the cell pellet washed with PBS. Cells were resuspended in 500µl of PBS, and then 4.5ml of 100% ethanol,

pre-cooled to 4°C, was added drop-wise, with continuous agitation. Fixed cells were stored at 4 °C until required.

In preparation for FACS analysis, the MRC5, C9 and C60 fixed cells were spun down (500rpm, 3 min), washed twice with PBS, then resuspended in 1ml of PBS containing 100µg/ml RNase and 10µg/ml of propidium iodide. FACS analysis was performed using the BD FACS Canto™ II flow cytometer with FACSDiva software.

Chapter 3: Results

3.1: Phosphorylation of CIP29

3.1.1. Analysis of CIP29 in response to double-strand breaks

Previous work by this laboratory has found the *X. laevis* ortholog of CIP29 to be a DNA DSB-dependent phosphorylation target of ATM. A high degree of conservation exists within eukaryotic DDR networks, therefore we considered it likely that human CIP29 also undergoes DNA damage-dependent phosphorylation. In order to investigate this possibility, MRC5-V1 cells were treated with two DNA DSB inducing agents, neocarzinostatin (NCS) and hydrogen peroxide (H_2O_2), and the CIP29 protein subsequently analysed by SDS-PAGE electrophoresis and Western blotting. Both NCS and H_2O_2 directly induce oxidative SSB lesions through free radical formation (Goldberg, 1987; Ward et al, 1985). The coincidental generation of SSBs in close proximity on opposing DNA strands then results in DSBs (Sage & Harrison, 2011).

MRC5-V1 cells were incubated in the presence or absence of $200\mu M H_2O_2$ or $10nM NCS$ at $37^\circ C$ for 1h. Total cell extracts for phospho-protein analysis were prepared, as described in section 2.2.1, and equivalent amounts were resolved by SDS-PAGE electrophoresis, and subjected to Western blotting by antibodies against CIP29, and the two controls, GAPDH and γ -H2AX. As Fig. 3.1-A shows, there was no significant difference in CIP29 protein levels following treatment with either DSB-inducing agent relative to the GAPDH loading control. The activity of the DNA damaging agents is confirmed by the increase in γ -H2AX following treatment with both H_2O_2 and NCS (Kuo & Yang, 2008).

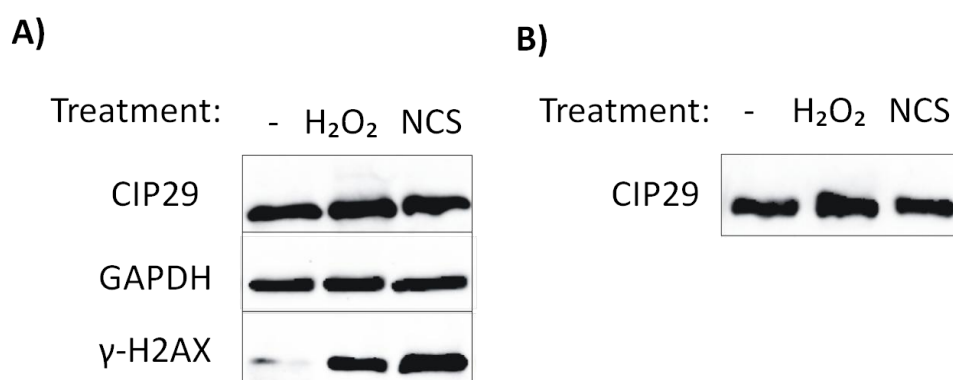


Fig 3.1 Western blots of untreated, and H_2O_2 and NCS-treated MRC5-V1 cell extracts, following resolution by **A)** normal SDS-PAGE or **B)** Phos-Tag™ gel electrophoresis.

In addition, there is no evidence of a reduced mobility form of CIP29 following DSB induction, which would have been consistent with protein phosphorylation. Many

phosphorylation events do not produce a readily detectable change in apparent molecular weight on conventional SDS-PAGE electrophoresis. Indeed, the damage-dependent phosphorylation of *X.laevis* Cip29 (XCip29) was not detectable on normal SDS-PAGE electrophoresis, and could only be detected using the Phos-Tag™ ligand. The acrylamide pendant Phos-Tag™ can be copolymerized with standard SDS-PAGE resolving gels, whereupon it acts as a phosphate-binding tag molecule. Phosphorylated proteins trapped by immobilized Phos-Tag™ in the resolving gel migrate more slowly, resulting in more efficient separation of phosphorylated proteins from their non-phosphorylated or less phosphorylated counterparts (Kinoshita et al, 2015). In light of the increased resolution of phosphoprotein isoforms offered by Phos-Tag™ gel analysis, the cell extracts from this experiment were also analysed using Phos-Tag™ SDS-PAGE gel electrophoresis, to determine whether a phosphorylated form of CIP29 could be detected using this technique. However, as Fig.3.1-B demonstrates, resolution of these cell extracts on a Phos-Tag™ gel, followed by immunoblotting, did not reveal any evidence of a DNA damage-induced mobility change for CIP29 suggestive of CIP29 phosphorylation. This may be because CIP29 is not phosphorylated in response to DNA damage in human cells, or alternatively, the conditions to detect DNA damage-induced phosphorylation of the human CIP29 protein through Phos-Tag™ gel analysis may need further optimization.

3.1.2. Phosphorylation of XCip29 in human cells

Since conditions have already been established for the detection of DNA damage-dependent phosphorylation of XCip29, we wondered whether it might be possible to detect phosphorylation of XCip29 when expressed in human cells. To this end, the XCip29 gene was PCR amplified using primers EP49 and EP50 and subcloned into a mammalian expression vector PCI-FF, in frame with a double FLAG epitope tag. The purified plasmid was transfected into MRC5-V1 cells, and then cells were incubated in the presence or absence of 5mM caffeine overnight. Caffeine is known to inhibit the catalytic activity of all three PI3KK kinases (ATM, ATR and DNA-PK) and consequently significantly impedes the DDR (Block et al, 2004; Sarkaria et al, 1999). Total cell extracts for phospho-protein analysis were generated. Equivalent amounts of each extract were resolved using Phos-Tag™ SDS-PAGE electrophoresis and the FLAG-tagged XCip29 protein was detected on a Western blot using the anti-FLAG antibody.

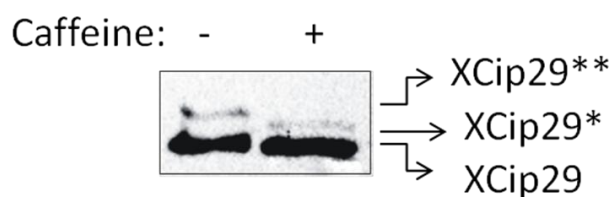


Fig 3.2 Western blots of MRC5-V1 cells transfected with XCip29 PCI-FF, and incubated in the presence or absence of caffeine.

In Fig 3.2, in addition to the main XCip29 band, a lower mobility form of XCip29 can be seen in the absence of caffeine (XCip29**), a finding consistent with protein phosphorylation. With caffeine treatment, this apparent phospho-protein isoform of CIP29 runs with a higher mobility on Phos-Tag™ gel, than in the absence of caffeine. This suggests that caffeine treatment has decreased the level of XCip29 phosphorylation, conceivably as a consequence of inhibition of the PI3KK kinases.

The results of this experiment therefore adds credibility to the previous laboratory finding that XCip29 is phosphorylated by the PI3K-related kinase ATM. However, this caffeine-dependent mobility shift of XCip29 proved difficult to reproduce. In light of this, it was decided not to pursue this strategy for detection of CIP29 phosphorylation. Instead, the focus of my research shifted to the characterisation of CIP29 knockout cell lines.

3.2. Characterisation of CIP29 Knockout cells

3.2.1. Generation of CIP29 mutant cells by CRISPR cloning

The function of CIP29 in human cells remains ambiguous, with minimal and even conflicting phenotypes reported in the literature (Choong et al, 2001; Fukuda et al, 2002; Leaw et al, 2004). Previous work by this laboratory has demonstrated that CIP29 is difficult to ablate through siRNA knockdown (Skelly, 2014). It is unclear whether the limited phenotypes described relate to redundancy of function, or whether they relate to a variable amount of CIP29 expression remaining after siRNA knockdown. Therefore, in order to more definitively investigate the phenotype resulting from CIP29 mutation, and thus establish potential functions for the protein, it was thought preferable to generate CIP29 mutant cell lines. Prior to the commencement of my research into CIP29, the CRISPR (clustered, randomly interspaced, short palindromic repeat)-Cas9 genome editing technique was used to produce two CIP29 mutant cell lines, C9 and C60.

The CRISPR-Cas system is a prokaryotic immune mechanism used to stop foreign genetic elements, predominantly viruses, from invading the host genome. The system incorporates fragments of foreign DNA, known as 'spacers' into its sequence, and then uses corresponding CRISPR RNAs (cRNAs) to guide degradation of homologous sequences by Cas endonucleases (Terns & Terns, 2011). The type II CRISPR-Cas system, which uses the Cas 9 effector endonuclease, has been employed to introduce RNA-guided genomic modifications into numerous eukaryotic organisms, and has revolutionized genome engineering biology. (Mali et al, 2013) To achieve this genome editing, Cas 9 is complexed with a specific small guide RNA (sgRNA) to form an RNA-guided endonuclease (RGEN) ribonucleoprotein, which is then able to target specific single, or even multiple gene sequences. The Cas 9 enzyme induces DSBs in the target sequence(s), which are then repaired, predominantly by error-free HR, but also by error-prone NHEJ. If misrepair occurs, in which nucleotides are inserted or deleted erroneously, the gene sequence can be knocked out of frame, preventing normal gene expression. Modified donor DNA can be used to help incorporate site-specific mutations into the sequence during HR. (Richter et al, 2013).

In the CRISPR genome editing of CIP29, the RGEN was targeted to exon 2 of the protein, as indicated in Fig 3.4. The CRISPR targeting construct was transfected into MRC5-V1 cells and that resulting colonies screened for lack of CIP29 expression using Western blotting. Two potential CIP29 mutant cell lines, designated C9 and C60 were identified, and these form the basis of characterisation experiments presented in this thesis.

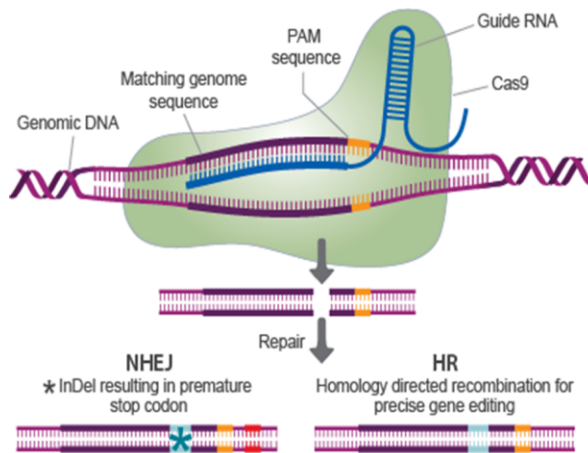


Fig 3.3 Diagram demonstrating the principles of CRISPR-Cas genome editing. The CRISPR-associated endonuclease Cas 9 is complexed to guide RNA, and then, through base-pairing between the guide RNA sequence and the genomic target sequence, is targeted to a specific gene region, where it then cleaves both strands of the genomic DNA, generating a DSB. The Cas 9 endonuclease will only cleave DNA strands 3-4 nucleotides 5' of a protospacer adjacent motif (PAM) sequence. The requirement for a PAM sequence adjacent to the targeted genomic DNA sequence prevents cleavage of the CRISPR locus itself by Cas 9 endonuclease. The DSB at the target site is then repaired by either NHEJ or HR. In NHEJ, insertions or deletions (InDels) often occur during the repair process, leading to frameshifts. In HR, homologous sequences containing precise mutations are incorporated into the sequence, thus disrupting the gene.

Image Citation: Transomic Technologies (2015) "CRISPR/Cas9 for Genome Editing". Transomic.com (online review).
<http://www.transomic.com/Products/CRISPR-Genome-Editing.aspx>
 Image reproduced with the permission of Transomic Technologies.

```

ggatctgggataataaagtggtaaggagaatctgcttttagatcattggattttctacttgaagggttcattcttcc
aatatgctggctgccacagtagtcttaagaaaaaaccttttccccctcagaatatttagaataaactagaga
tttgtgacagttagtaggatatacaaatagatgaggtttttattaaagtgtgatgtttattcttcagcatctgtt
aggcagttcctcttgtatattgaatatcgttagaggaaaatggatcatcttgtggacctagagccttggtagaa
ttaaggcagtaatttgggatggaacttcattttcttttttcttttcttctgtgggaactaccattttattcact
ggtgtcatcctgttaactaaggaaaagttttatttttttccccctcagcttgccgaactaaagcaagaatgtctt
gctcgtggtttggagaccaaggggaataaagcaagatcttatccacagactccaggcatatctgaagaacatggt
gagtactttgtggaggcggagtgatgtgagtgaggggattttcaggctttgacactgaaaagatttctttttttt
tttcaggtcatttagcaatgtaagctcttaattaacggcatcaagaaaactctcttttttttttttttggatgg
agtcttgetctgttggccaggctggagtgcagtgcagcagtttcagctcattgcaacctctgtctcccggcttca
accaattctcctgtctcagcctcccaagcagctgggactacaggcgagcaccacatgcctggctgatttttgta
tttttagtagagacggggtttcaccatattggttgggctggtctagaattcctgacctcaggtgagccaccgccc
tcagcctcccaaagtgtggtgattacagtgtgtgagccaccgcgcccagccatcttgtacaacctacatcttag
  
```

Fig 3.4 CIP29 genomic DNA surrounding exon 2, shown from PCR primer EP42 to PCR primer EP41 (highlighted in blue). Exon 2 is highlighted in yellow, and the CRISPR targeted sequence, in red.

3.2.2. Absence of CIP29 expression in the CIP29 mutant cell lines, C9 and C60

To confirm that expression of CIP29 had been abolished in the two putative cell lines, C9 and C60, cell extracts for total protein analysis were generated from MRC5-V1, C9 and C60 cells and equivalent amounts resolved by SDS-PAGE electrophoresis. The extracts were subjected to Western blotting by CIP29, and the loading control GAPDH.

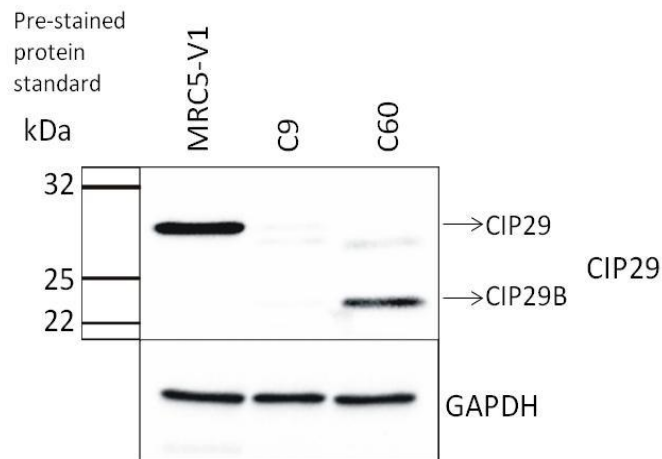


Fig 3.5 Western blots of MRC5-V1, C9 and C60 cell extracts, incubated with CIP29 and GAPDH. The bands of the pre-stained protein standard have been shown at their approximate levels in relation to the protein bands.

Fig 3.5 shows a protein band (at approximately 29kDa) reflective of normal CIP29 expression in the MRC5-V1 wild-type cells. By contrast, in the C9 and C60 cell lines the full-length CIP29 protein is barely discernible, indicating that normal CIP29 gene expression is effectively abolished in these CRISPR-generated clones. However, in the C60 cell extract, a lower CIP29 cross-reacting band (approximately 23kDa) can clearly be seen (CIP29_B). It may be that CRISPR genome editing has resulted in a truncated form of CIP29 being produced by the C60 cells. This may have implications for interpreting the phenotypes exhibited by the two CIP29 knockout cell lines, as C60 cells may express a residual amount of mutated CIP29 protein, whereas C9 cells almost entirely lack CIP29 expression.

3.2.3. Sequencing of the CIP29 mutant cell lines

To identify the CIP29 mutations which abolished CIP29 expression in the C9 and C60 cell lines, it was decided to sequence the CIP29 gene in the region targeted by CRISPR-Cas genome editing. This was achieved by PCR amplification of a 923bp region of genomic DNA sequence surrounding exon 2, followed by sequencing of the resulting PCR products. Genomic DNA was generated from MRC5-V1, C9 and C60 cells. As Fig 3.6 shows, the genomic DNA generated from the MRC5-V1, C9, and C60 cells was intact and not subject to extensive degradation. The region of genomic DNA around exon 2 was then PCR amplified

with primers EP41 and EP42, as described in section 2.1.2. Water was used as a negative control.

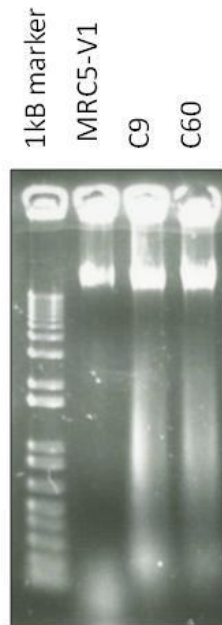


Fig 3.6 MRC5-V1, C9 and C60 genomic DNA run on a 0.8% agarose gel, alongside a 1kB marker.

As Fig 3.7 A) shows, PCR performed on the MRC5-V1 genomic DNA generated a PCR product of the expected size at approximately 920 bp. The PCR reaction performed on C60 genomic DNA also generated a PCR band at around 920 bp, and, in addition, a second, lower band (of approximately 700bp). We hypothesized that this lower band may represent a CRISPR-targeted allele of CIP29 which has undergone a more extensive deletion, and may give rise to the truncated form of CIP29 (CIP29_B) that was earlier visualized on Western blotting of the C60 mutant cell line. No PCR product was obtained from amplification of the C9 genomic DNA. To characterise the two C60 PCR band products, both the higher and lower C60 DNA bands were gel purified (Fig 3.7 B)) and then cloned into pGEM-Teasy™ vector, along with the wild type PCR product derived from MRC5-V1 cells.

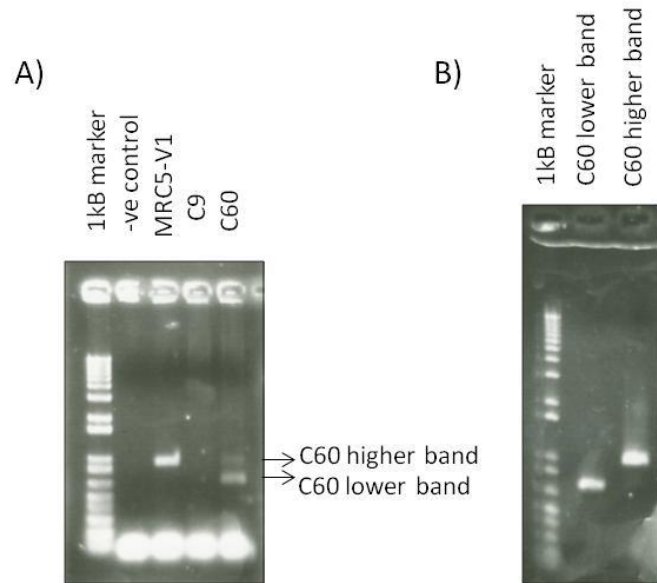


Fig 3.7 Agarose gel images of: A) The negative control, MRC5-V1 C9 and C60 PCR products and B) The C60 lower band and higher band products.

Plasmids containing the various PCR products were identified by restriction digest with EcoR1. DNA sequencing was then performed on one plasmid containing the CIP29 exon 2 sequence derived from MRC5-V1, two plasmids containing the C60 940bp amplification product, and five samples containing the C60 700bp amplification product.

All of the five C60 700bp plasmids were found to contain a large deletion of 246 bp in the middle of the PCR amplified CIP29 gene sequence (see Fig 3.8). This sizeable deletion was shown to entirely encompass exon 2.

```

ggatctgggataataagtggtaaggagaatctgcttttagatcattggatcttctacttgaaggttcattcttcc
aatatgctggctgccacagtagtcttaagaaaaaaccttttccccctcagaatatttagaaataactagaga
tttgtgacagttagtaggtatacaaatagatgaggttttttattaaagtgtgatgtttattcttcagcatctggt
aggcagttcctcttgatattgaatatcgttagaggaaaatggatcatctttgtggacctagagccttggtagaa
ttaagggcagtaatttgggatggaacttcattttctttttttcttttccttgtgggaactaccattttattcact
ggtgttcatcctgttaactaaggaaaagttttattttttttcccctcagcttgccgaactaagcaaggaatgtctt
gagcaaggaatgtcttgggttgggagaccaaggaataaaagcaagatcttatccacagactccaggcatacttgaagaacatggt
gagtactttgtggaggcggagtgatgtgagtgaggggattttcaggctttgacactgaaaagatttctttttttt
ttttcaggtcattagcaatgtaagctcttaattaacggcatcaagaaaactctctcttttttttttttgagatgg
agtcttgcctctgttgccaggctggagtgcagtgacgcagtttcagctcattgcaacctctgtctcccggcttca
accaattctcctgtctcagcctcccaagcagctgggactacaggcgagcaccaccatgcttggtgatTTTTGTA
TTTTAGTAGAGACGGGTTTCCACATATTGGTTGGGCTGGTCTAGAATTCCTGACCTCAGGTGAGCCACCGCC
tcagcctcccaaagtgtctgggattacagttgtgagccaccgcgccagccatcttgtacaacctacatcttag

```

Fig 3.8 Genomic DNA of the C60 cell line from PCR primer EP42 to PCR primer EP41 (highlighted in blue). Exon 2 is highlighted in yellow, and the CRISPR targeted sequence in red. The section of gene sequence deleted by CRISPR gene editing in the lower band of the C60 cell line is in orange text.

As Fig 3.9 demonstrates, deletion of exon 2, which contains 100bp, from the CIP29 DNA sequence produces a frameshift mutation, resulting in an altered amino acid sequence, and a premature stop codon. mRNA produced from transcription of this mutated CIP29 gene would likely undergo nonsense-mediated decay, and thus CIP29 expression would not occur.

A) Wild-type CIP29

```
M A T E T V E L H K L K L A E L K Q E C L A R G L E T K G I K Q D L I H R L Q A Y L E E H  
A E E E A N E E D V L G D E T E E E E T K P I E L P V K E E P P E K T V D V A A E K K V  
V K I T S E I P Q T E R M Q K R A E R F N V P V S L E S K K A A R A A R F G I S S V P T K  
G L S S D N K P M V N L D K L K E R A Q R F G L N V S S I S R K S E D D E K L K K R K E R  
F G I V T S S A G T G T T E D T E A K K R K R A E R F G I A
```

B) Lower band CIP29

```
M A T E T V E L H K L K L A E L K Q E C L K R R Q M K K M Y W E M K Q R K K K Q S P L  
S S L S K R K N P L K K L L M W Q Q R R K W Stop
```

Fig 3.9 Figure showing the amino acid sequence of wild-type CIP29, and the amino acid sequence of the CRISPR-generated C60 lower band fragment. The deletion of the DNA sequence of exon 2 has resulted in a frameshift mutation, causing different amino acids to appear in the sequence, and a premature stop codon.

It appears likely that the mutation in this C60 lower band fragment would prevent expression of the CIP29 protein, and therefore seems that this allele would not in fact give rise to the truncated form of CIP29 (CIP29_B) that was identified on Western blotting of the C60 cell line.

Sequencing of the two plasmids containing the 920bp PCR products derived from C60 revealed two differing gene sequences, containing deletions of 16 bp and 10bp respectively (see Fig 3.10)

```

MRC5      TACCATTTTATTCACTGGTGTTCATCCTGTTAACTAAGGAAAAGTTTATTTTTTTTCCCC
HB1       TACCATTTTATTCACTGGTGTTCATCCTGTTAACTAAGGAAAAGTTTATTTTTTTTCCCC
HB2       TACCATTTTATTCACTGGTGTTCATCCTGTTAACTAAGGAAAAGTTTATTTTTTTTCCCC
*****

MRC5      TCAGCTTGCCGAACTAAAGCAAGAATGTCTTGCTCGTGGTTTGGAGACCAAGGGAATAAA
HB1       TCAGCTTGCCGAACTAAAGCAAGA-----TTGGAGACCAAGGGAATAAA
HB2       TCAGCTTGCCGAACTAAAGCAAGAATGTCTTGC-----GAGACCAAGGGAATAAA
*****

MRC5      GCAAGATCTTATCCACAGACTCCAGGCATATCTTGAAGAACATGGTGAGTACTTTGTGGA
HB1       GCAAGATCTTATCCACAGACTCCAGGCATATCTTGAAGAACATGGTGAGTACTTTGTGGA
HB2       GCAAGATCTTATCCACAGACTCCAGGCATATCTTGAAGAACATGGTGAGTACTTTGTGGA
*****

```

Fig 3.10 Section of the gene sequence from the wild-type MRC5 cells, and the two 940bp C60 plasmids , HB1 and HB2. HB1 contains a deletion of 16bp, and HB2 a deletion of 10bp. A star beneath a particular base indicates that it is the same in all three sequences.

In both HB1, and HB2, both deletions generated frameshift mutations. These mutations resulted in altered amino acids in the sequence, and premature stop codons within exon 2. The mRNA produced from these mutated genes would probably undergo nonsense-mediated decay, and therefore expression of the CIP29 protein would not occur.

```

WT   LAELKQECLARGLETGKGIKQDLIHLRLQAYLEEH
HB1  LAELKQDWRPRE Stop
HB2  LAELKQECLARPRE Stop

```

Fig 3.11 The amino acid sequence of wild-type CIP29 exon 2, and the amino acid sequences of the two CRISPR generated C60 fragments, HB1 and HB2. The HB1 plasmid has a deletion of 16 base pairs, and the HB2 plasmid, a deletion of 10 base pairs. In both, the deletions have resulted in frameshift mutations, causing different amino acids to be appear in the sequence, and premature stop codons.

It is apparent that CRISPR genome editing has resulted in three different alleles of the CIP29 gene in the C60 cells. This may indicate a possible gene duplication of CIP29 in these cells. In one allele a substantial deletion of 246 bp has occurred, producing a frameshift mutation in the CIP29 gene sequence and likely abolished CIP29 expression. In the other two alleles, smaller deletions, of 16 and 10 bp respectively, have been induced, also leading to frameshift mutations in the gene sequence, and probable abolished CIP29 expression. We have been unable to identify a C60 allele that would account for the truncated protein product (CIP29_B) identified on Western blotting.

Unfortunately, repeated attempts to generate a PCR product from the C9 genomic DNA were unsuccessful. We are currently unable to explain why this was the case. As Fig 3.6 shows, the C9 genomic DNA did not appear to be significantly more degraded than either the C60 or MRC5-V1 genomic DNA, and so we do not consider the quality of the template to be the likely cause of the problem. One possibility is that CRISPR-Cas9 genome editing resulted in a deletion affecting one of the primer annealing sites, therefore preventing successful PCR reactions. Future work is required to try and overcome this problem, and sequence CIP29 in the C9 mutant cell line.

3.2.4. Assessment of CIP29 mutant cell proliferation

Previous research, by Fukuda et al, found the CIP29 protein to be expressed at higher levels in rapidly dividing tissues, such as myeloid leukaemia and lymphoma cell lines, while in UT7/Epo leukaemic cells, CIP29 expression was found to be enhanced by both Epo stimulation, and treatment with a growth factor cocktail known to promote early stem and progenitor cell proliferation. Furthermore, it was discovered that increased CIP29 expression resulted in a greater proportion of UT7/Epo cells progressing to the S or G2/M cell cycle phases, whereas reduced CIP29 expression led to a progressive exit from the cycle (Fukuda et al, 2002).

In light of this research, suggesting a potential role for CIP29 in cell proliferation and/or cell cycle control, we decided to investigate the impact of CIP29 mutation on cell proliferation using a metabolic cell proliferation assay.

Metabolic cell proliferation assays are a recognized way of evaluating the number of cells in a culture that are dividing at a given time. The activity of NADPH-dependent cellular oxidoreductase enzymes within the culture is representative of the number of dividing cells, and can be quantified using a tetrazolium dye reagent. When applied to the culture medium, tetrazolium dyes are reduced by NADPH-dependent cellular oxidoreductase enzymes, forming formazan dyes, and producing a colour change of the medium. The amount of formazan dye can then be measured using a plate reader.

Proliferation assays were carried out on MRC5-V1 cells and the C9 and C60 mutant cell lines, according to the method outlined in section 2.3.7. For each experiment, average readings for each cell line and time point were calculated from three wells. The entire assay was repeated three times. The average of these three independent experiments is present in Fig 3.12.

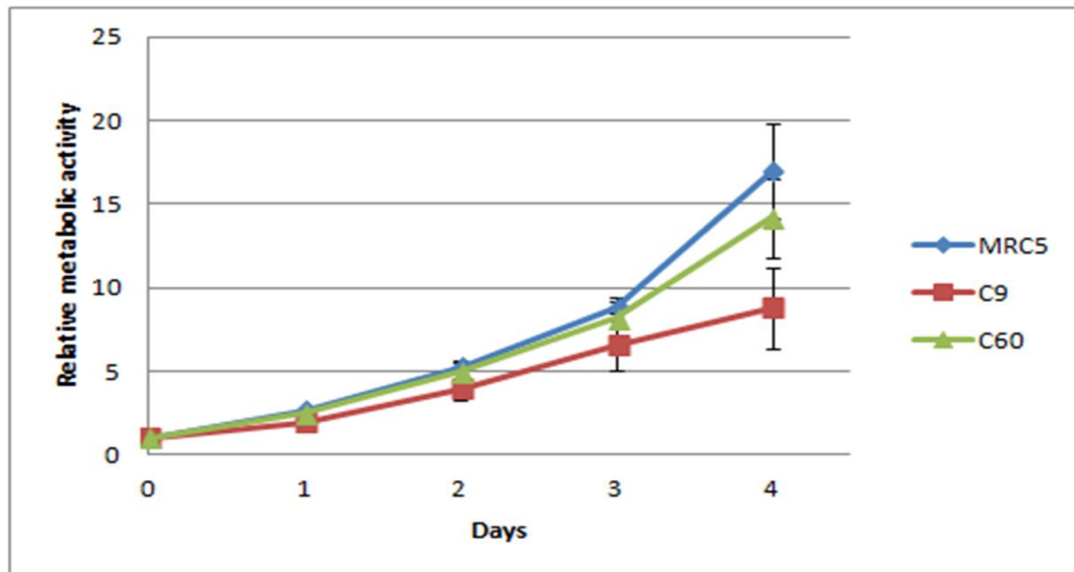


Fig 3.12 Graph, showing the proliferation rates of MRC5-V1 C9 and C60 cells over 4 days. The average values from three independent experiments are presented where error bars represent SEM.

As Fig 3.12 demonstrates, the growth rate of the C60 cells is very slightly but reproducibly reduced, relative to parental MRC5-V1 cells, while the proliferation rate of C9 cells is more significantly affected. The decreased proliferation rates of the mutant cell lines, may signify a role for CIP29 in cell proliferation, consistent with other reports, although in the case of the C60 it seems that this effect is small. The significant difference in proliferation rates observed between the C9 and C60 cell lines has several possible explanations. Firstly, the C60 cells could express a truncated form of the CIP29 protein (CIP29_B), and therefore the phenotype observed in this cell line may not be representative of full CIP29 knockout. In the C9 cell line, no expression of any form of CIP29 was detected, so it may be that the significantly reduced proliferation rate observed in this cell line truly reflects the impact of CIP29 knockout on cellular proliferation.

Secondly, it is possible that an off-target effect of CRISPR cloning has arisen in the C9 cell line, and that the considerably decreased proliferation rate in this cell line is a consequence of this, and not exclusively the result of CIP29 mutation.

3.2.5 Metaphase spread analysis of CIP29 mutant cell lines

In a study looking at the mRNA export factors UAP56 and URH49, siRNA knockdown of both CIP29 and its interacting protein URH49 was reported to cause chromosome arm resolution

defects. The arms of a sister chromatid usually become separated during prophase and prometaphase stages of the cell cycle (Onn et al, 2008), but in the CIP29 and URH49 knockdown cell lines, they appeared to remain attached, or 'closed'. In the URH49 knockdown cell line, 70% of metaphases displayed a closed arm phenotype, relative to 25-30% in the control cells. In the CIP29 knockdown cells however the closed arm phenotype was observed with only slightly increased frequency: 50% of metaphases displayed a closed arm phenotype in the CIP29 knockdown cells relative to the 25-30% seen in the control cells. This indicates that CIP29 may only be partially required to prevent such chromosome arm resolution defects, or alternatively that the siRNA knockdown did not sufficiently abolish CIP29 expression. (Yamazaki et al, 2010)

We hypothesized that the slowed proliferation rate observed in the CIP29 mutant cell lines could be the result of a mitotic progression defect. We therefore chose to investigate chromosome segregation in the CIP29 mutant cell lines, based on the assay developed by Yamazaki et al. Since we were using cells with abolished expression of the complete CIP29 protein, rather than knockdown cell lines, we hoped we would overcome any issues associated with incomplete siRNA knockdown of expression, and perhaps would see a more extensive defect in chromosome arm resolution.

Since a variety of methods for metaphase chromosome spreading have been described (Deng et al, 2003), initially, it was necessary to optimise the chromosome spreading technique used. Four chromosome spreading techniques were trialled, to determine the technique that both maximized the number of visible metaphases per slide, and also ensured clear visualization of individual chromosomes by adequately separating them out within metaphases.

MRC5-V1 cells were treated with colcemid (10ng/ml) for 2h. Cell suspensions were then generated, by treating cells with ten-fold diluted (0.005%) trypsin/EDTA. It was thought that treatment with diluted 0.005% trypsin/EDTA could give a lower background of non-mitotic cells on chromosome spreading. These cell suspensions were then swollen in hypotonic KCl solution and fixed and washed with a 3:1 solution of methanol: glacial acetic acid, as described in section 2.3.10.

A glass slide was then prepared from the fixed cell suspensions using each of the four chromosome spreading techniques outlined below:

Technique one:

A glass slide was rinsed in fix solution, and briefly air dried. The slide was then breathed on, and 40µl of cell suspension was immediately dropped onto it from a height of ~ 10cm. Five drops of fix solution were immediately pipetted on top, and the slide gently tilted (x10) , before being stood up to drain. As the cells became visible (after approx. 10s) two to three further drops of fix were dropped onto the slide, which was then left to air dry.

Technique two:

Four to five drops of cell suspension were dropped onto a wet glass slide, previously stored in water at 4°C. The slide was propped up and when the droplets ran off, two to three drops of fix were dropped on top. The slide was stood up, and the edge blotted to remove excess fix. When the fix began to evaporate, the slide was placed on a 45°C heat block to dry.

Technique three:

A metal plate was placed at the surface of a 55°C water bath, and allowed to warm. A glass slide was placed on the metal plate, allowed to warm for 2 mins and then one or two drops of cell suspension were dropped onto the slide from a height of ~5cm. The water bath was covered for 2 minutes, to maintain a humid atmosphere, then the slide was removed and air-dried.

Technique four:

A glass slide was held face down for 10s, over water that had been microwaved, until condensation appeared. 20µl of cell suspension was immediately pipetted onto the slide, and spread evenly across the surface using the pipette tip. When, after 10-20s the slide surface appeared grainy, the slide was briefly held over the water again, and then placed on a 40°C hot plate to dry.

After Giemsa™ staining, all 4 slides were examined using light microscopy. Five widely dispersed fields on each slide were selected, and the number of metaphases visible in each field was counted. Then, an overall score from 1 to 5 was given to each field to describe how spread out the chromosomes in the metaphases were, with 1 indicating that the chromosomes were on top of each other, and 5 meaning that the chromosomes were so spread out it was impossible to tell which metaphase they came from. In an ideal situation, there would be many metaphases visible in all fields, and they would receive a score of 3 or 4 for degree of chromosome spread.

Technique	Average no. of metaphases per field	Average spread of the chromosomes (1-5)
1	10.8	2.8
2	34.2	2.2
3	34.4	1.4
4	14.8	1

Table 3.1 Table showing the average number of metaphases per field, and the average degree of chromosome spread, for each chromosome spreading technique.

On examination of these results, it was apparent that the four chromosome spreading techniques produced varying numbers of metaphases, with techniques 2 and 3 generating significantly higher numbers. Similarly, wide variation in the average spread of the chromosomes within these metaphases was observed, with techniques 3 and 4 producing metaphases in which the chromosomes were too close together to be distinguished from one another. It was ultimately decided to adopt chromosome spreading technique 1, because it produced an adequate number of metaphases, with the chromosomes well separated.

In order to accurately recapitulate the assay carried out by Yamazaki et al, it was decided that each cell line would be treated with Colcemid (10ng/ml) for 6 hours.

Once the best conditions for chromosome spreading had been ascertained, chromosome spreading of MRC5-V1, C9 and C60 cells was performed, and the glass slides stained with DAPI mounting solution. Fluorescent microscopy was then used to visualize 200 metaphases, and judge whether each exhibited a 'closed' or 'open' arm phenotype.

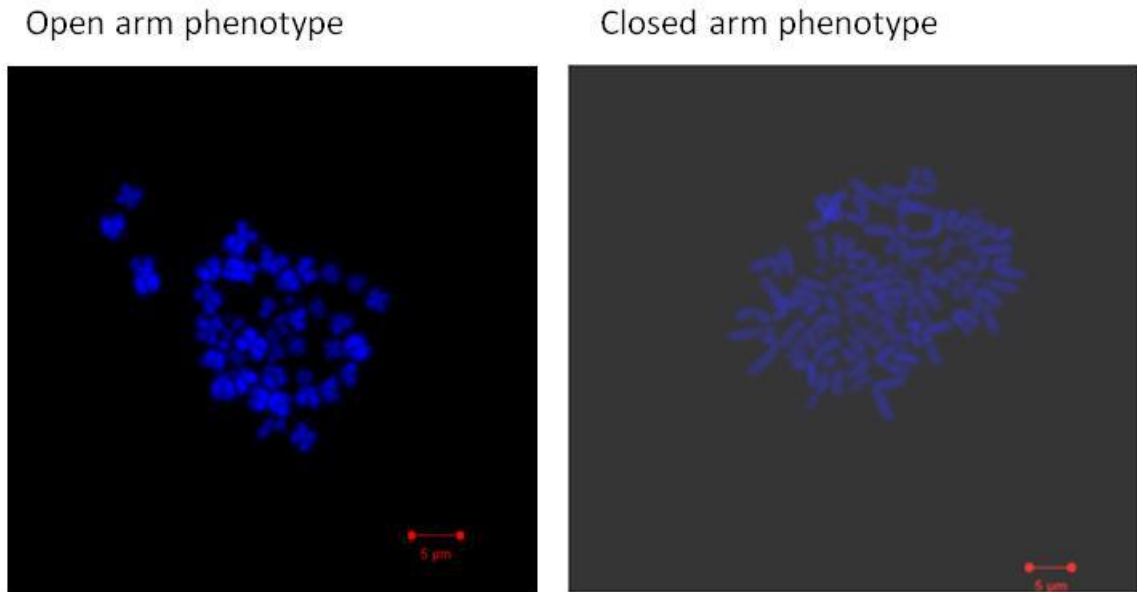


Fig 3.13 Diagram demonstrating an open arm and closed arm phenotype.

	MRC5-VI	C9	C60
Open arm phenotype	155	153	151
Closed arm phenotype	45	47	49

Table 3.2 Table showing the number of open and closed arm phenotypes observed in 200 metaphases from the MRC5-VI, C9 and C60 cell lines.

As table 3.2 shows, in the three cell lines, MRC5-V1, C9 and C60 there was very little difference between the numbers of metaphases displaying an open arm or closed arm phenotype. Contrary to the research by Yamazaki et al, the two CIP29 mutant cell lines did not display a significantly increased frequency of chromosome arm resolution defects, when compared to the wild-type cells. It appears therefore that our CIP29 mutant cells do not demonstrate chromosome arm resolution defects.

3.2.6. Cell cycle analysis of CIP29 mutant cells

Since we could not detect any obvious chromosome arm segregation defect, we decided to further investigate the perturbed proliferation of the C9 and C60 cells, through Fluorescent Advanced Cell Sorting (FACS) analysis, which would determine the proportion of cells in each cell cycle phase at a particular time point. It was hoped that this would highlight whether CIP29 mutant cells exhibit an altered rate of progression through any particular cell cycle

phase, which may then shed light on the reason for the reduced proliferation rates exhibited by the CIP29 mutant cells.

MRC5-V1, C9 and C60 cells were fixed and stained with propidium iodide as described (section 2.3.11) and cell cycle analysis was performed.

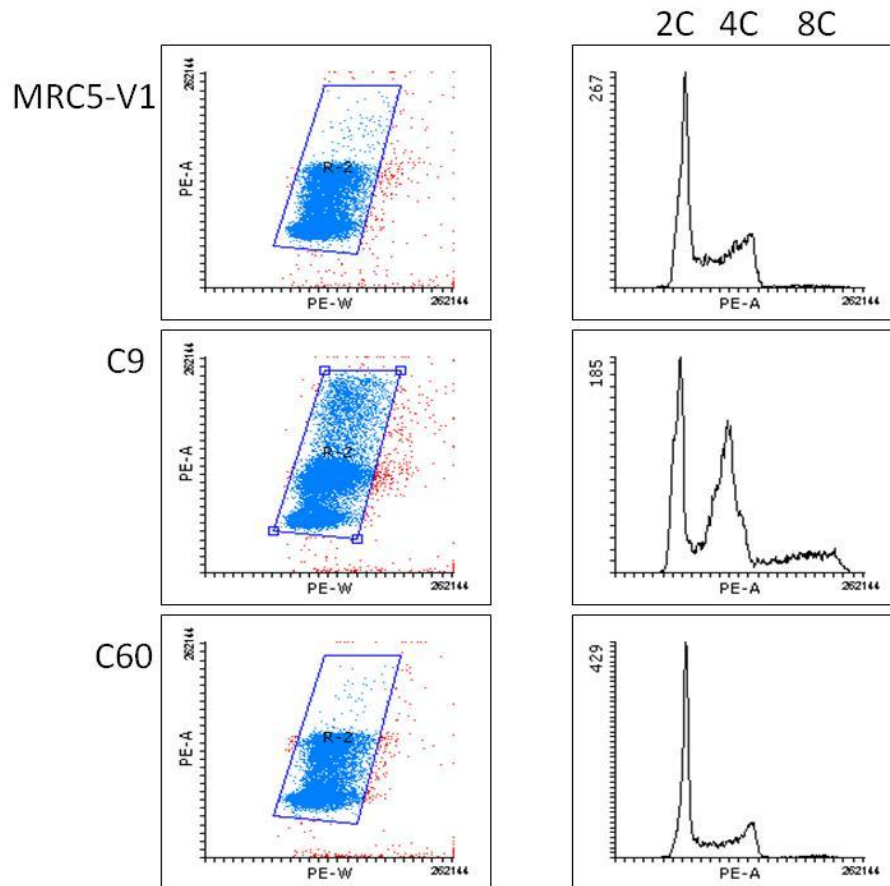


Fig 3.14 The results from FACS analysis carried out on the MRC5-V1, C9 and C60 cell lines. The graphs on the left shows the width of the cells (x axis) versus the area (y axis). The gate R-2 has been applied to exclude doublet cells (seen as red dots) from the cell cycle analysis. The graphs on the right demonstrate the progression through the cell cycle of MRC5-V1 , C9 and C60 cells.

The FACS analysis revealed some interesting findings about the cell cycle of the CIP29 mutant cells. There does not appear to be a substantial difference in the proportion of the cell population in each phase of the cell cycle in the C60 and wild-type cells. However, it could be argued that there is a slight decrease in the proportion of cells in the S and G2/M phases of the cycle in the C60 cells relative to the wild-type cells, which could explain the slightly decreased proliferation rate of the C60 cells.

In the C9 cells, a much higher proportion of the cells are in the G2/M phase of the cell cycle, relative to wild-type and C60 cells. This indicates some form of disruption of progression through this cell cycle phase. Additionally, there is the appearance of an 8C population in the C9 cells. This indicates that a proportion of the cells have undergone DNA replication, acquiring a 4C DNA content, but then division of these cells into two new daughter cells has not occurred, and the cells have then undergone a second round of DNA replication, acquiring an 8C DNA content. Furthermore, on the accompanying C9 dot-plot, a population of cells with a similar width, but increased PI signal intensity can be seen. The heightened PI intensity indicates that these cells contain increased amounts of DNA. Taken together, these findings suggest that the C9 cells have a defect in cytokinesis, the process by which the cytoplasm of two daughter cells is physically separated at the end of mitosis. This could explain the more significantly decreased proliferation rate observed in the C9 cells.

3.2.7. Sensitivity of CIP29 mutant cells to etoposide and camptothecin

Earlier research from this laboratory showed CIP29 to be a DNA-damage dependent target of ATM. We were therefore interested to see whether abolishing CIP29 expression would increase cellular sensitivity to DNA damaging agents. Cytotoxicity assays using the DNA damaging agents etoposide and camptothecin were carried out to ascertain whether the CIP29 knockout cells demonstrated any altered sensitivity to these agents, relative to MRC5-V1 cells. If mutation of CIP29 made the cells more sensitive to etoposide, camptothecin or both, this would suggest a role for CIP29 in the DDR to treatment with these agents. Conversely, if the C9 and C60 cell lines exhibited reduced sensitivity to either or both of the agents, this would suggest a survival advantage in cells depleted of CIP29, and indicate that CIP29 in some way impedes the DDR to treatment with either or both drugs.

Etoposide and camptothecin are commonly used chemotherapeutic agents which both work by inhibiting the activity of DNA topoisomerase enzymes. For many biological processes, such as DNA replication, transcription and recombination, to occur, the two strands of the DNA helix must separate, allowing access to the genetic information. Unwinding of the DNA helix is executed by DNA topoisomerases enzymes, which also have roles in relaxing supercoiled DNA and separating intertwined chromosomes during cell division. Type I topoisomerases function by passing a strand of DNA through a single-strand break in the opposing DNA strand, whereas type II topoisomerases pass a duplex region of DNA through a double-strand break in the DNA (Champoux, 2001).

In order to maintain the integrity of the DNA sequence and allow efficient re-ligation of the cleaved DNA ends during this process, the strand breaks induced by both types of topoisomerase enzyme are held together by covalent phosphotyrosyl bonds, termed 'cleavage complexes'. In low numbers, cleavage complexes are generally well-tolerated by cells, but in elevated numbers, they can induce frameshift mutations, permanent DSBs, and even trigger apoptosis (Burden et al, 1996).

A variety of topoisomerase-targeting chemotherapeutic drugs have been developed, most of which prevent re-ligation of the cleavage complexes, and consequently promote apoptosis of cancerous cells. (Champoux, 2001) Etoposide inhibits topoisomerase II, preventing re-ligation of DSBs introduced by the enzyme (Burden et al, 1996). Camptothecin stabilizes topoisomerase I-cleavage complexes, which can then block DNA replication and transcription, leading to fork stalling and conversion of the SSB-associated cleavage complexes to DSBs (Liu et al, 2000).

In order to determine the cellular sensitivity of CIP29 mutant cells to etoposide/camptothecin, a cytotoxicity assay was performed as described in section 2.3.8. In this assay, cells were treated with varying concentrations of either of the two DNA damaging agents, and, after a certain time period, the extent of cellular proliferation was determined. MRC5-V1, C9 and C60 cells were grown in the presence of 0, 100, 500 and 1000nM camptothecin, and 0, 5, 10, 20 μ M of etoposide, for 3 days, and then a metabolic cell proliferation assay was used to measure cellular proliferation.

Average readings for each cell line and drug dose were calculated.

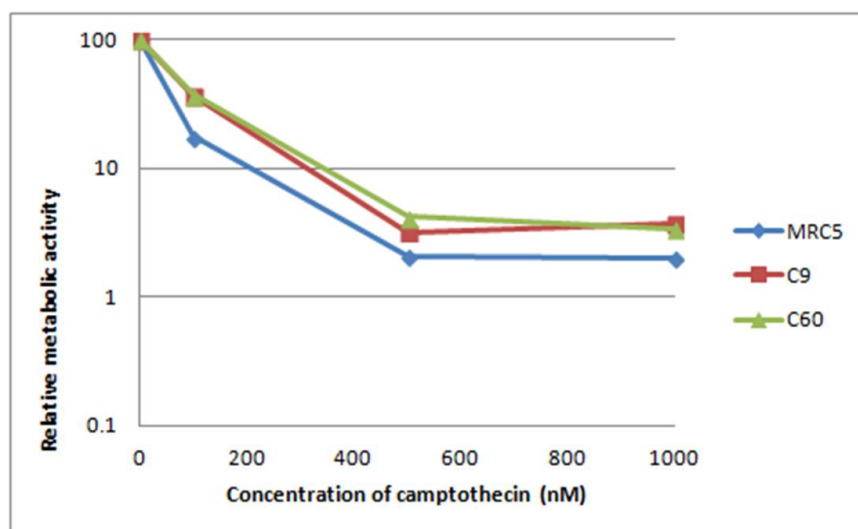


Fig 3.15 Graph showing the sensitivity of MRC5-V1 C9 and C60 cells to camptothecin (0-1000nM).

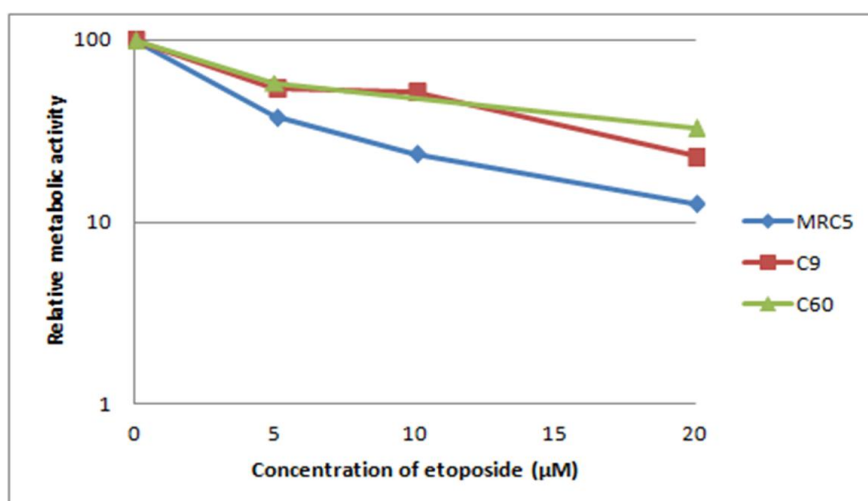


Fig 3.16 Graph showing the sensitivity of MRC5-V1,C9 and C60 cells to etoposide (0-20µM).

As Fig 3.15, and Fig 3.16 show, neither the etoposide nor the camptothecin cytotoxicity assay demonstrated a substantial difference in survival rates between MRC5-V1 wild type cells, and the CIP29 mutant cells, C9 and C60. In fact, the two CIP29 mutant cell lines do appear to display a very slight degree of resistance to both etoposide and camptothecin, relative to the parental MRC5-V1 cell line. However, these observations are both based upon a single experiment, and further work is required to confirm the reproducibility of this data.

3.2.8. Sensitivity of CIP29 Knockout cells to Neocarzinostatin

To extend our investigations into the sensitivity of CIP29 mutant cells to DNA damaging agents, a clonogenic survival assay was carried out on the MRC5-V1, C9 and C60 cell lines following treatment with the DSB-inducing agent, NCS. NCS is a naturally occurring enediyne antibiotic and potent mutagen, which exerts its genotoxic activity by intercalating with DNA, and generating free radicals, which consequently induces both single and double-stranded DNA lesions (Chin et al, 2012).

To assess sensitivity to NCS, MRC5-V1, C9 and C60 cells were incubated in 0, 5, 10, and 15nM NCS for 1h, then the drug was removed. Cells were plated at varying cell densities and grown under standard conditions for 10 days to allow colony formation. Colonies were subsequently stained and counted, and clonogenic cell survival was determined for each cell line and drug concentration, relative to an untreated control.

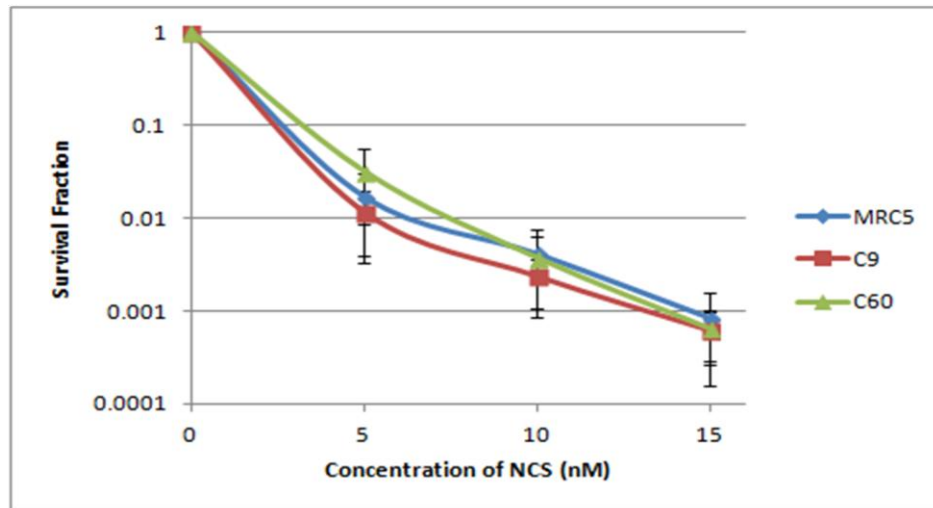


Fig 3.17 Graph showing the sensitivity of MRC5-V1, C9 and C60 cells to NCS, established by a clonogenic survival assay. The averages from three separate experiments are presented, where the errors bars represent SEM.

In the NCS clonogenic survival assay, as seen in Fig 3.20, the three cell lines, MRC5-V1, C9 and C60 demonstrated similar survival fractions when treated with each concentration of NCS. The C9 and C60 cells did not demonstrate increased sensitivity to NCS compared to wild-type cells.

3.2.9 Generation of CIP29 stable transfectant cell lines

In order to ascertain whether the phenotypes observed in our CIP29 mutant cell lines were actually due to reduced CIP29 expression and not, for example, due to off-target effects of the CRISPR gene editing, it will be essential to demonstrate that the phenotypes can be reversed by restoration of CIP29 expression. To this end, we decided to generate stable transfectants of the C9 and C60 cell lines, in which CIP29 expression was restored.

CIP29 was cloned into the mammalian expression vectors PCI-neo and PCI-FF (PCI-neo containing a double FLAG epitope tag.)

Subsequently, PCI Neo (vector only control), CIP29-PCI Neo, CIP29-PCI-FF plasmids were transfected into MRC5-V1, C9 and C60 cells and grown under selection (800µg/ml G418) to allow colony formation by stably transfected cells and stable transfectants were then isolated. Confirmation that CIP29 expression has been restored in these stable transfectants and subsequent phenotypic analysis will be a priority for future laboratory research into CIP29.

Chapter 4: Discussion

The DNA damage response (DDR) is a global signalling network dedicated to maintaining genome integrity by identifying DNA damage, eliciting cell cycle arrest, activating DNA repair pathways, or, if cells are irreparably damaged, triggering apoptosis (Jackson & Bartek, 2009). The ATM protein kinase is one of three major PI3KK kinases involved in co-ordinating the molecular response to DNA damage. ATM is activated mainly in response to DNA DSBs, but is also phosphorylated in response to oxidative base damage (Paull, 2015), and the formation of R-loops (Tresini et al, 2015). Once phosphorylated, ATM phosphorylates a number of downstream effector proteins which then orchestrate an effective DDR. A recent proteomic analysis revealed that RBPs involved in various processes, such as mRNA splicing, RNA modification, RNA export and translation make up a significant proportion of ATM's substrates (Matsuoka et al, 2007). A functional interplay between RNA processing and the DDR has recently been recognised, and a number of mechanisms by which RBPs function to uphold genomic stability have been described (Wickramasinghe & Venkitaraman, 2016). RBPs can control DDR gene expression through alternative splicing of mRNA, control of transcription elongation and regulation of mRNA export. Certain RBPs play essential roles in preventing the formation of R-loops, or in their resolution. Additionally, a number of RBPs have been identified as having specific roles in the DDR itself.

The protein CIP29, which is over-expressed in both solid-organ and haematological cancers (Fukuda et al, 2002), is thought to potentially be an RBP with involvement in mRNA export. Knockdown of CIP29 has been shown to inhibit export of mRNA from the nucleus, and CIP29 has been reported to interact with either UAP56 or URH49 to form an mRNA export complex, which may be involved in maintaining mRNP biogenesis (Dufu et al, 2010; Yamazaki et al, 2010). From yeast studies, it seems that this function may be especially important in the absence of the THO subcomplex (Jimeno et al, 2006b). Several studies have suggested some involvement of CIP29 in the control of cell proliferation, possibly by influencing cell cycle progression (Fukuda et al, 2002; Leaw et al, 2004). Furthermore, siRNA knockdown of the protein was reported to result in a chromosome arm resolution defect, leading to the idea that it may play some role in the control of mitosis (Yamazaki et al, 2010). Previous research from this laboratory focusing on *X.laevis* Cip29, found that the protein is phosphorylated in response to DNA DSBs, and that this phosphorylation is dependent upon the activity of ATM (Holden, 2014). The major damage-dependent phosphorylation site on XCip29 was identified

as Ser 95. Unusually, this Ser residue is not at an S/T-Q site, which is the typical consensus site for ATM phosphorylation, however this residue is conserved in the human CIP29 protein, suggesting that the human protein may be similarly targeted after DNA damage. The purpose of my research was to examine the function of human CIP29, with a particular focus on whether CIP29 serves as a target and/or functional component of the DDR in human cells.

4.1: DNA-damage dependent phosphorylation of CIP29 in human cells

A number of potential phosphorylation sites have been predicted for CIP29, but so far only three of these, Ser115, Ser162 and Ser163 have been verified as phosphorylation targets in phosphoproteomic screens (Dephoure et al, 2008; McNulty & Annan, 2008; Olsen et al, 2010). DNA-damage dependent phosphorylation of CIP29 has not previously been described. Nevertheless, on the basis of previous research from this laboratory, we anticipated that CIP29 would be phosphorylated in response to DSBs for several reasons. Firstly, a high degree of conservation exists within eukaryotic DDR networks. Secondly, XCip29 and CIP29 share a high degree of homology: they possess a 72% identical genetic sequence. Orthologs typically perform comparable roles in their respective organisms, and a high degree of homology, as in this case, is thought to increase the probability that they will function similarly (Hulsen et al, 2006; Peterson et al, 2009; Tatusov et al, 1997). Moreover, the residue identified as the phospho-acceptor site on XCip29, Ser 95, is conserved in the human CIP29 protein. However, despite enhancing the sensitivity of our SDS-PAGE electrophoresis method with the addition of the Phos-Tag™ ligand, we were unable to detect a phosphorylation shift of CIP29 in response to DSBs. We suggest that, despite the increased resolution of phosphoprotein isoforms gained by using the Phos-Tag™ ligand, the SDS-PAGE electrophoresis technique used was still not sensitive enough to detect a CIP29 phosphorylation shift. Although we could not detect CIP29 phosphorylation using this technique, neither can we rule out the possibility of damage-dependent CIP29 phosphorylation on this basis. There are limitations to use of Phos-Tag™: not all phospho-isoforms will give rise to a mobility shift on a gel even with the addition of the Phos-Tag™ ligand (Kinoshita et al, 2009), and the technique is very sensitive to variations in both Phos-Tag™ concentration and protein loading (Barbieri & Stock, 2008).

Although we could not detect phosphorylation of human CIP29 under these conditions, we were able to detect phosphorylation of XCip29 when expressed in human cells. This phosphorylation shift was altered following caffeine treatment, indicating that at least some component of the phosphorylation of XCip29 in human cells is dependent on PI3KK activity. Treatment of the cells with a specific ATM kinase inhibitor would be needed to confirm whether this phosphorylation is specifically dependent on ATM kinase activity in human cells, as it is in *X.laevis* egg extracts.

In recent years, mass spectrometry has emerged as the most powerful technique both for identifying phosphoproteins, and identifying phosphorylation sites. The technique is extremely sensitive, capable of detecting phosphosites within a single protein or a complex mixture of multiple proteins (Gafken, 2009). Employing mass spectrometry to try and detect damage-dependent phosphorylation of human CIP29 would be the logical next step to extend our research into CIP29 phosphorylation.

4.2: Confirmation of CIP29 mutated cell lines

Previous studies into CIP29 have made inferences about the function of the protein by characterising siRNA CIP29 knockdown cells. However, it is not clear if the limited phenotypes described in these studies truly reflect lack of CIP29 expression, or if they are the result of a variable amount of CIP29 expression remaining despite siRNA knockdown. It was therefore decided to use CRISPR-genome editing to generate and then characterise CIP29 mutant cell lines, which could give a greater insight into possible functions of CIP29. Two potential CIP29 mutant cell lines, C9 and C60 were produced by a CRISPR construct targeted to exon 2.

Western blotting confirmed that CIP29 expression was abolished in the C9 cell line. In the C60 cell line, although no full length CIP29 is produced, a smaller form of the protein, at approximately 23kDa is expressed. Sequencing of the targeted CIP29 gene from the C60 mutant cell line identified three different alleles of CIP29 in this cell line. In all of these alleles, frameshift mutations had been induced, introducing premature termination codons and thereby abolishing CIP29 expression. We could not identify an allele which would account for the smaller protein band (CIP29_B) seen on Western blotting of the C60 cell line. It might be suggested that the CIP29_B protein, judging by its lower molecular weight (23kDa compared to the 29kDa full-length CIP29 protein) may have a significant region of the protein missing. However, the C60 cell line did not demonstrate a significant reduction in

functionality compared to wild-type cells e.g. there was no significant reduction in cellular proliferation, or increased sensitivity to DNA damaging agents. This may suggest that whatever the deleted region of CIP29 protein in CIP29_B, it is largely dispensable for the function of the protein. Future laboratory work could employ reverse transcription PCR (RT-PCR) to identify the DNA sequence which has resulted in the CIP29_B protein and thus identify any mutations and their consequent impact on the CIP29 amino acid sequence.

For reasons that are not yet clear, we were unable to verify the CIP29 mutation(s) introduced by CRISPR genome editing in the C9 cell line, despite repeated attempts to PCR amplify exon 2 from several different preparations of C9 genomic DNA. It is possible that none of the C9 genomic DNA preparations was of good enough quality to be successfully PCR amplified. Alternatively, a relatively large deletion may have been induced following CRISPR targeting, affecting one of the PCR primer annealing sites, thereby preventing PCR amplification. Nevertheless, it is clear from Western blotting that CIP29 expression is effectively abolished in this cell line.

4.3: Proliferation and cell cycle progression of the CIP29 mutant cell lines

Various studies have presented somewhat conflicting findings about the involvement of CIP29 in cellular proliferation and the cell cycle. It was therefore decided to try to ascertain the exact role of CIP29 in cell proliferation and cell cycle control by carrying out a proliferation assay using our CIP29 knockout cells. The assay revealed a slightly reduced rate of proliferation of the C60 cells relative to the MRC5-V1 cells, but a more significantly decreased rate in the C9 cells.

In light of the suggested involvement of the AREX complex (CIP29-URH49) in mitotic progression (Yamazaki et al, 2010), it was decided to try and ascertain whether the reduced proliferation rates observed in the CIP29 cells could be the result of a mitotic progression defect. Yamazaki et al. described an increase in chromosome arm resolution defects in URH49 knockdown cells: 70% of metaphases demonstrated a closed arm phenotype in these cells relative to 25-30% in control cells. They also described a slightly increased frequency of chromosome arm resolution defects in CIP29 siRNA knockdown cells (50% closed arm phenotype compared to 25-30% in control cells) but we predicted that due to the complete absence of CIP29 expression, these defects might be more extensively observed in our knockout cell lines. However, we were unable to detect any appreciable difference in

numbers of metaphases demonstrating closed arm and open arm phenotypes in the C9 and C60 cell lines relative to wild-type cells. It is unclear why our results did not replicate the findings of Yamazaki et al. It is possible that the increased frequency of chromosome arm resolution defects seen in the URH49 and CIP29 knockdown cells in Yamazaki et al's study were the result of off-target effects of siRNA knockdown. Silencing of unintended transcripts by siRNAs is widespread and can be problematic in functional genetic studies (Jackson et al, 2003).

Since our metaphase spread analyses did not reveal any mitotic defect, we subsequently decided to perform FACS analysis on the wild-type, C9 and C60 cells, to try and ascertain the cause of the reduced proliferation rates in the CIP29 mutant cells. The proportion of cells in each stage of the cell cycle appeared to be pretty comparable in the MRC5-V1 and C60 cells, with perhaps a minor decrease in the proportion of C60 cells in the S and G2/M phases. This could explain the slightly reduced proliferation rate in the C60 cells.

In the C9 cells, an increased proportion of cells were in the G2/M phase of the cycle compared to both the wild-type and C60 cells. Additionally, an 8C population of cells, indicative of tetraploidy, was seen. The dot-plot revealed a proportion of cells with similar width but increased PI intensity, indicative of an increased amount of DNA in these cells. These findings were strongly suggestive of a cytokinesis defect in the C9 cells.

Cytokinesis is the final step in cell division, during which the cell cytoplasm is separated, producing two daughter cells. It consists of four highly regulated stages (Normand & King, 2010). The process is initiated when the key cytokinesis regulator RhoA specifies the cleavage plane. In the second stage, the cleavage furrow ingresses. In the third stage, which requires central spindle proteins, the cleavage furrow is stabilized, and the mid-body is formed. The final stage is abscission, in which the cytoplasmic contents are separated from one another. Progression to the next stage of cytokinesis is dependent upon correct execution of the prior stage; therefore cytokinesis failure can result if there is interference with any of the four stages.

Cytokinesis is predominantly regulated by mitotic protein kinases, including Cdks, Polo kinase (Plk1) and the Aurora B kinase complex. Disruption to the activity of any of these three regulatory kinases can result in defective cytokinesis. Both Plk1 and the Aurora B complex play positive roles in cytokinesis regulation. Plk1 is involved recruitment and activation of RhoA (Burkard et al, 2007), and may also be involved in phosphorylating central

spindle proteins, such as MKLP2 (Neef et al, 2003) and NudC (Nishino et al, 2006). The Aurora B kinase complex activates several proteins, including MKLP1, which may be involved in stabilizing the mid-body and recruiting proteins involved in abscission (Guse et al, 2005), and MgcRacGAP, which is thought to terminate RhoA activity in the later phases of cytokinesis (Minoshima et al, 2003). Both Plk1 and Aurora B have been shown to be over-expressed in multiple cancers (Chieffi et al, 2006; Smith et al, 2005; Sorrentino et al, 2005; Strebhardt & Ullrich, 2006; Tatsuka et al, 1998).

Contrastingly, Cdk1 plays a generally inhibitory role in cytokinesis. Inactivation of Cdk1 via cyclin destruction catalyzed by the Anaphase-Promoting Complex/Cyclosome (APC/C) is essential for cytokinesis to begin. Cdk1 prevents cytokinesis via a number of mechanisms. Cdk1 activity impedes the RhoA pathway (Yüce et al, 2005), hinders central spindle formation (Normand & King, 2010), and phosphorylates both PRC1 and MKLP1, reducing their affinity for microtubules (Mishima et al, 2004; Mollinari et al, 2002). However, Cdk1-dependent phosphorylation is actually essential for some aspects of cytokinesis: it sets up the Plk1-dependent phosphorylation that occurs early in cytokinesis, and is also important in recruiting essential cytokinesis proteins like Nir2 and Cep55. (Fabbro et al, 2005; Litvak et al, 2004).

Cytokinesis failure can result in polyploidy, a state in which a cell contains more than one set of chromosomes (Storchova & Pellman, 2004). When polyploid cells enter the cell cycle, they may be detected by the polyploidy checkpoint, and consequently undergo p53-mediated cell cycle arrest in the G1 phase, followed by apoptosis (Andreassen et al, 2001). Cells that escape this checkpoint can enter multipolar mitosis, resulting in aneuploidy, the state in a cell contains an abnormal number of chromosomes. Aneuploid cells commonly contain chromosomal aberrations, and their production has been linked to increased genomic instability and tumorigenesis (Lingle et al, 1998; Sato et al, 1999; Storchova & Pellman, 2004; Weber et al, 1998; Yamamoto et al, 2009). The DDR employs a number of mechanisms, aside from the polyploidy checkpoint, to try and avoid aneuploidy, mainly by preventing proliferation of genetically unstable cells. The SAC prevents chromosome missegregation in mitosis, thus lessening the risk of aneuploidy (Li & Zhang, 2009), and an Aurora-B controlled checkpoint, modulated by Chk1, acts to prevent furrow regression in cells with abnormal chromosome segregation (Peddibhotla et al, 2009; Steigemann et al, 2009).

The defect seen in the C9 CIP29 mutant cell line implicates CIP29 in the highly regulated cytokinesis process. Interestingly, Yamazaki et al. did describe a very slightly increased frequency of cytokinesis failure (2.5% increased frequency of binucleate cells) in the CIP29 knockdown cells relative to wild-type cells (Yamazaki et al, 2010). In our C9 mutant cells, CIP29 expression was shown to be completely abolished, whereas in the CIP29 siRNA knockdown cells, CIP29 expression may not have been completely knocked down. This could explain the more convincing appearance of a cytokinesis defect in our C9 mutant cells. The nature of CIP29's involvement in cytokinesis is unclear. Previous work by this laboratory investigated whether XCip29 phosphorylation might be cell-cycle dependent (Holden, 2014). Experiments using *Xenopus* egg extract revealed the appearance of a modified form of XCip29 during mitosis, suggesting that cell cycle-dependent XCip29 phosphorylation does occur, and could be under mitotic regulation. A putative Cdk phosphorylation site, Ser 162, was identified on the XCip29 amino acid sequence, further suggesting that XCip29 undergoes cell cycle-dependent phosphorylation. In G2/M *Xenopus* extract, XCip29 phosphorylation was shown to positively correlate with Cdk1 activity, leading to the suggestion that the XCip29 phosphorylation could be Cdk1-dependent. It may be that Cdk dependent phosphorylation of CIP29 occurs during mitosis, with the CIP29 protein then playing some sort of role in promoting completion of cytokinesis. It is perhaps noteworthy that CIP29, like Plk1 and the Aurora B kinase, which have positive regulatory roles in cytokinesis, is upregulated in several cancers. Since CIP29 has been implicated in mRNA export, one possibility may be that CIP29 regulates cytokinesis through upregulating the export of mRNAs coding for proteins involved in the process. Alternatively, CIP29 could play a role in signalling the end of mitosis and start of cytokinesis.

To further investigate the role of CIP29 in cytokinesis, it would be useful to perform binucleate immunofluorescence screening on our C9 CIP29 knockout cells to ascertain the proportion of binucleate cells and thus infer from this the extent of cytokinesis failure. Further, we need to ascertain whether CIP29 undergoes mitotic, Cdk-dependent phosphorylation, and the outcomes of such phosphorylation. We could also investigate whether CIP29 localizes to cytokinesis apparatus such as the cleavage furrow or midbody. It would also be valuable to identify proteins associated with CIP29 to determine whether it forms connections with other proteins involved in cytokinesis, or in mRNA export. This could potentially be achieved by using the protein ligase Bir A, which when fused to a protein of interest, biotinylates nearby proteins that can then be pulled down by streptavidin-coated beads and identified by mass spectrometry (Roux et al, 2012).

4.4: Sensitivity of the knockout cell lines to DNA-damaging agents

Given that XCip29 was shown to be phosphorylated in response to DNA DSBs, it was decided to assess the sensitivity of the two CIP29 mutant cell lines to NCS, a DSB-inducing agent. Our NCS clonogenic survival assay did not reveal any altered sensitivity of the C9 and C60 cell lines to NCS, in comparison to wild-type cells. This indicates that CIP29 does not play a crucial role in maintain cell survival following the induction of DSBs, and hence that it appears not to be involved in the DDR to DSBs.

Similarly, single etoposide and camptothecin sensitivity assays did not show any substantial difference in sensitivity of the CIP29 mutant cells compared to wild-type cells. However, a very mild increase in resistance was seen in both the C9 and C60 cell lines. Both camptothecin and etoposide induce DSBs through inhibition of the topoisomerase enzymes: camptothecin inhibits topoisomerase I (Liu et al, 2000), and etoposide, topoisomerase II (Burden et al, 1996). Since these enzymes induce DSBs during the cell cycle, particularly during DNA replication, it could be that as the cellular proliferation rate has been shown to be reduced in both the C9 and C60 cell lines, less damage has been incurred in these cell lines compared to the wild-type cells, resulting in the slightly increased resistance to etoposide and camptothecin. However, since the etoposide and camptothecin sensitivity assays were both only performed once, they would need to be repeated to ascertain whether the slight resistance observed in the C9 and C60 cells is genuine or simply an experimental error. This would be a priority for future research into CIP29.

4.5: Conclusion

The purpose of this thesis was to investigate the functions of the human CIP29 protein. A primary focus of our research was to ascertain whether CIP29 is a target of the DDR. We were unable to detect phosphorylation of CIP29 in response to DNA DSBs. Furthermore, the two CRISPR-generated CIP29 mutant cell lines did not show significantly altered sensitivity to DNA damaging agents compared to wild-type cells. These findings suggest that human CIP29 does not play an important functional role in the DDR, but mass spectrometry should be employed to definitively ascertain whether CIP29 undergoes damage-dependent phosphorylation.

Examination of the cellular proliferation rates of the CIP29 mutant cell lines demonstrated a slightly reduced proliferation rate in the C60 cell line, but a substantially reduced rate in the C9 cells. Metaphase spread analysis did not reveal any mitotic defect in either the C60 or C9 cell lines. FACS analysis demonstrated a very mild decrease in the proportion of cells in the S and G2/M phases in the C60 cells compared to wild-type, which might explain the slightly decreased proliferation rate in this cell line. By contrast, the FACS analysis revealed significant evidence of a cytokinesis defect in the C9 cell line, thus implicating CIP29 in the execution of cytokinesis. This finding is interesting as no substantial link between CIP29 and cytokinesis has been described previously. Future work is needed to ascertain what role, if any, CIP29 plays in this process.

References

Adamson B, Smogorzewska A, Sigoillot FD, King RW, Elledge SJ (2012) A genome-wide homologous recombination screen identifies the RNA-binding protein RBMX as a component of the DNA-damage response. *Nature Cell Biology* **14**: 318-328

Aguilera A (2005) mRNA processing and genomic instability. *Nature Structural & Molecular Biology* **12**: 737-738

Andreassen PR, Lohez OD, Lacroix FB, Margolis RL (2001) Tetraploid state induces p53-dependent arrest of nontransformed mammalian cells in G1. *Molecular Biology of the Cell* **12**: 1315-1328

Aravind L, Koonin EV (2000) SAP – a putative DNA-binding motif involved in chromosomal organization. *Trends in Biochemical Sciences* **25**: 112-114

Bakkenist CJ, Kastan MB (2003) DNA damage activates ATM through intermolecular autophosphorylation and dimer dissociation. *Nature* **421**: 499-506

Banin S, Moyal L, Shieh S, Taya Y, Anderson CW, Chessa L, Smorodinsky NI, Prives C, Reiss Y, Shiloh Y, Ziv Y (1998) Enhanced phosphorylation of p53 by ATM in response to DNA damage. *Science* **281**: 1674-1677

Barbieri CM, Stock AM (2008) Universally applicable methods for monitoring response regulator aspartate phosphorylation both in vitro and in vivo using Phos-tag™ based reagents. *Analytical biochemistry* **376**: 73-82

Bartek J, Lukas C, Lukas J (2004) Checking on DNA damage in S phase. *Nature Reviews Molecular Cell Biology* **5**: 792-804

Basu U, Meng FL, Keim C, Grinstein V, Pefanis E, Eccleston J, Zhang T, Myers D, Wasserman CR, Wesemann DR, Januszyk K, Gregory RI, Deng H, Lima CD, Alt FW (2011) The RNA exosome targets the AID cytidine deaminase to both strands of transcribed duplex DNA substrates. *Cell* **144**: 353-363

Bennett M, Pinol-Roma S, Staknis D, Dreyfuss G, Reed R (1992) Differential binding of heterogeneous nuclear ribonucleoproteins to mRNA precursors prior to spliceosome assembly in vitro. *Molecular Cell Biology* **12**: 3165-3175

Bensimon A, Schmidt A, Ziv Y, Elkon R, Wang SY, Chen DJ, Aebersold R, Shiloh Y (2010) ATM-dependent and -independent dynamics of the nuclear phosphoproteome after DNA damage. *Science Signaling* **3**: 2001034

Bhatia V, Barroso SI, Garcia-Rubio ML, Tumini E, Herrera-Moyano E, Aguilera A (2014) BRCA2 prevents R-loop accumulation and associates with TREX-2 mRNA export factor PCID2. *Nature* **511**: 362-365

Blazek D, Kohoutek J, Bartholomeeusen K, Johansen E, Hulinkova P, Luo Z, Cimermancic P, Ule J, Peterlin BM (2011) The Cyclin K/Cdk12 complex maintains genomic stability via regulation of expression of DNA damage response genes. *Genes and Development* **25**: 2158-2172

Block WD, Merkle D, Meek K, Lees-Miller SP (2004) Selective inhibition of the DNA-dependent protein kinase (DNA-PK) by the radiosensitizing agent caffeine. *Nucleic Acids Res* **32**: 1967-1972

Boucas J, Riabinska A, Jokic M, Herter-Sprue GS, Chen S, Hopker K, Reinhardt HC (2012) Posttranscriptional regulation of gene expression-adding another layer of complexity to the DNA damage response. *Frontiers in Genetics* **3**

Burden DA, Kingma PS, Froelich-Ammon SJ, Bjornsti MA, Patchan MW, Thompson RB, Osheroff N (1996) Topoisomerase II. etoposide interactions direct the formation of drug-induced enzyme-DNA cleavage complexes. *Journal of Biological Chemistry* **271**: 29238-29244

Burkard ME, Randall CL, Larochelle S, Zhang C, Shokat KM, Fisher RP, Jallepalli PV (2007) Chemical genetics reveals the requirement for Polo-like kinase 1 activity in positioning RhoA and triggering cytokinesis in human cells. *Proceedings of the National Academy of Sciences of the United States of America* **104**: 4383-4388

Cao L, Alani E, Kleckner N A pathway for generation and processing of double-strand breaks during meiotic recombination in *S. cerevisiae*. *Cell* **61**: 1089-1101

Champoux JJ (2001) DNA topoisomerases: structure, function, and mechanism. *Annual Review of Biochemistry* **70**: 369-413

Chan YA, Hieter P, Stirling PC (2014) Mechanisms of genome instability induced by RNA-processing defects. *Trends in Genetics : TIG* **30**: 245-253

Chaudhary MW, Al-Baradie RS (2014) Ataxia-telangiectasia: future prospects. *Journal of the Application of Clinical Genetics* **7**: 159-167

Chaudhuri J, Alt FW (2004) Class-switch recombination: interplay of transcription, DNA deamination and DNA repair. *Nature Reviews Immunology* **4**: 541-552

Chen BP, Uematsu N, Kobayashi J, Lerenthal Y, Krempler A, Yajima H, Lobrich M, Shiloh Y, Chen DJ (2007) Ataxia telangiectasia mutated (ATM) is essential for DNA-PKcs phosphorylations at the Thr-2609 cluster upon DNA double strand break. *Journal of Biological Chemistry* **282**: 6582-6587

Chi B, Wang Q, Wu G, Tan M, Wang L, Shi M, Chang X, Cheng H (2013) Aly and THO are required for assembly of the human TREX complex and association of TREX components with the spliced mRNA. *Nucleic Acids Research* **41**: 1294-1306

Chieffi P, Cozzolino L, Kisslinger A, Libertini S, Staibano S, Mansueto G, De Rosa G, Villacci A, Vitale M, Linardopoulos S, Portella G, Tramontano D (2006) Aurora B expression directly correlates with prostate cancer malignancy and influence prostate cell proliferation. *Prostate* **66**: 326-333

Chin DH, Li HH, Kuo HM, Chao PD, Liu CW (2012) Neocarzinostatin as a probe for DNA protection activity--molecular interaction with caffeine. *Molecular Carcinogenesis* **51**: 327-338

Choong ML, Tan LK, Lo SL, Ren EC, Ou K, Ong SE, Liang RC, Seow TK, Chung MC (2001) An integrated approach in the discovery and characterization of a novel nuclear protein over-expressed in liver and pancreatic tumors. *FEBS Letters* **496**: 109-116

Cimprich KA, Cortez D (2008) ATR: an essential regulator of genome integrity. *Nature Reviews Molecular Cell Biology* **9**: 616-627

Cortez D (2005) Unwind and slow down: checkpoint activation by helicase and polymerase uncoupling. *Genes and Development* **19**: 1007-1012

de la Cruz J, Kressler D, Linder P (1999) Unwinding RNA in *Saccharomyces cerevisiae*: DEAD-box proteins and related families. *Trends in Biochemical Sciences* **24**: 192-198

Deng J, Harding HP, Raught B, Gingras A-C, Berlanga JJ, Scheuner D, Kaufman RJ, Ron D, Sonenberg N (2002) Activation of GCN2 in UV-Irradiated Cells Inhibits Translation. *Current Biology* **12**: 1279-1286

Deng W, Tsao SW, Lucas JN, Leung CS, Cheung ALM (2003) A new method for improving metaphase chromosome spreading. *Cytometry Part A* **51A**: 46-51

Dephoure N, Zhou C, Villen J, Beausoleil SA, Bakalarski CE, Elledge SJ, Gygi SP (2008) A quantitative atlas of mitotic phosphorylation. *Proceedings of the National Academy of Sciences of the USA* **105**: 10762-10767

Dominguez-Sanchez MS, Barroso S, Gomez-Gonzalez B, Luna R, Aguilera A (2011) Genome instability and transcription elongation impairment in human cells depleted of THO/TREX. *PLOS Genetics* **7**: 1

Dufu K, Livingstone MJ, Seebacher J, Gygi SP, Wilson SA, Reed R (2010) ATP is required for interactions between UAP56 and two conserved mRNA export proteins, Aly and CIP29, to assemble the TREX complex. *Genes & Development* **24**: 2043-2053

Dutertre M, Lambert S, Carreira A, Amor-Gu ret M, Vagner S (2014) DNA damage: RNA-binding proteins protect from near and far. *Trends in Biochemical Sciences* **39**: 141-149

Dutertre M, Sanchez G, De Cian M-C, Barbier J, Dardenne E, Gratadou L, Dujardin G, Le Jossic-Corcus C, Corcos L, Auboeuf D (2010) Cotranscriptional exon skipping in the genotoxic stress response. *Nature Structural Molecular Biology* **17**: 1358-1366

Fabbro M, Zhou BB, Takahashi M, Sarcevic B, Lal P, Graham ME, Gabrielli BG, Robinson PJ, Nigg EA, Ono Y, Khanna KK (2005) Cdk1/Erk2- and Plk1-dependent phosphorylation of a centrosome protein, Cep55, is required for its recruitment to midbody and cytokinesis. *Developmental Cell* **9**: 477-488

Falck J, Mailand N, Syljuasen RG, Bartek J, Lukas J (2001) The ATM-Chk2-Cdc25A checkpoint pathway guards against radioresistant DNA synthesis. *Nature* **410**: 842-847

Fu XD, Ares M, Jr. (2014) Context-dependent control of alternative splicing by RNA-binding proteins. *Nature Reviews Genetics* **15**: 689-701

Fukuda S, Wu DW, Stark K, Pelus LM (2002) Cloning and Characterization of a Proliferation-Associated Cytokine-Inducible Protein, CIP29. *Biochemical and Biophysical Research Communications* **292**: 593-600

Gafken PR (2009) An overview of the qualitative analysis of phosphoproteins by mass spectrometry. *Methods in Molecular Biology* **527**: 159-172

Gan W, Guan Z, Liu J, Gui T, Shen K, Manley JL, Li X (2011) R-loop-mediated genomic instability is caused by impairment of replication fork progression. *Genes and Development* **25**: 2041-2056

Gardiner M, Toth R, Vandermoere F, Morrice NA, Rouse J (2008) Identification and characterization of FUS/TLS as a new target of ATM. *Biochemical Journal* **415**: 297-307

Ginno P, Lott P, Christensen H, Korf I, Ch din F (2012) R-Loop Formation Is a Distinctive Characteristic of Unmethylated Human CpG Island Promoters. *Molecular Cell* **45**: 814-825

Goldberg IH (1987) Free radical mechanisms in neocarzinostatin-induced DNA damage. *Free Radical Biology and Medicine* **3**: 41-54

Gomez-Gonzalez B, Garcia-Rubio M, Bermejo R, Gaillard H, Shirahige K, Marin A, Foiani M, Aguilera A (2011) Genome-wide function of THO/TREX in active genes prevents R-loop-dependent replication obstacles. *Embo J* **30**: 3106-3119

Groh M, Lufino MM, Wade-Martins R, Gromak N (2014) R-loops associated with triplet repeat expansions promote gene silencing in Friedreich ataxia and fragile X syndrome. *PLOS Genetics* **10**

Guo Z, Deshpande R, Paull TT (2010) ATM activation in the presence of oxidative stress. *Cell Cycle* **9**: 4805-4811

Guse A, Mishima M, Glotzer M (2005) Phosphorylation of ZEN-4/MKLP1 by aurora B regulates completion of cytokinesis. *Current Biology* **15**: 778-786

Holden J (2014) Characterisation of Cip29: A novel target of the eukaryotic DNA damage response B.Sc. (Hons) Thesis, Biomedical and Life Sciences Lancaster University

Huertas P, Aguilera A (2003) Cotranscriptionally formed DNA:RNA hybrids mediate transcription elongation impairment and transcription-associated recombination. *Molecular Cell* **12**: 711-721

Hulsen T, Huynen MA, de Vlieg J, Groenen PM (2006) Benchmarking ortholog identification methods using functional genomics data. *Genome Biology* **7**: 13

Jackson AL, Bartz SR, Schelter J, Kobayashi SV, Burchard J, Mao M, Li B, Cavet G, Linsley PS (2003) Expression profiling reveals off-target gene regulation by RNAi. *Nature Biotechnology* **21**: 635-637

Jackson SP, Bartek J (2009) The DNA-damage response in human biology and disease. *Nature* **461**: 1071-1078

Jacobsen JOB, Allen MD, Freund SMV, Bycroft M (2016) High-resolution NMR structures of the domains of *Saccharomyces cerevisiae* Tho1. *Acta Crystallographica Section F, Structural Biology Communications* **72**: 500-506

Jimeno S, Luna R, Garcia-Rubio M, Aguilera A (2006a) Tho1, a novel hnRNP, and Sub2 provide alternative pathways for mRNP biogenesis in yeast THO mutants. *Mol Cell Biol* **26**: 4387-4398

Jimeno S, Luna R, Garcia-Rubio M, Aguilera A (2006b) Tho1, a novel hnRNP, and Sub2 provide alternative pathways for mRNP biogenesis in yeast THO mutants. *Molecular Cell Biology* **26**: 4387-4398

Jimeno S, Rondon AG, Luna R, Aguilera A (2002) The yeast THO complex and mRNA export factors link RNA metabolism with transcription and genome instability. *Embo J* **21**: 3526-3535

Jurado AR, Tan D, Jiao X, Kiledjian M, Tong L (2014) Structure and Function of Pre-mRNA 5'-End Capping Quality Control and 3'-End Processing. *Biochemistry* **53**: 1882-1898

Kai M (2016) Roles of RNA-Binding Proteins in DNA Damage Response. *International Journal of Molecular Sciences* **17**

Kastan MB, Zhan Q, el-Deiry WS, Carrier F, Jacks T, Walsh WV, Plunkett BS, Vogelstein B, Fornace AJ, Jr. (1992) A mammalian cell cycle checkpoint pathway utilizing p53 and GADD45 is defective in ataxia-telangiectasia. *Cell* **71**: 587-597

Katahira J (2012) mRNA export and the TREX complex. *Biochimica et Biophysica Acta (BBA) - Gene Regulatory Mechanisms* **1819**: 507-513

Kee Y, D'Andrea AD (2012) Molecular pathogenesis and clinical management of Fanconi anemia. *The Journal of Clinical Investigation* **122**: 3799-3806

Keskin H, Shen Y, Huang F, Patel M, Yang T, Ashley K, Mazin AV, Storici F (2014) Transcript-RNA-templated DNA recombination and repair. *Nature* **515**: 436-439

Khanna KK, Jackson SP (2001) DNA double-strand breaks: signaling, repair and the cancer connection. *Nature Genetics* **27**: 247-254

Kim ST, Lim DS, Canman CE, Kastan MB (1999) Substrate specificities and identification of putative substrates of ATM kinase family members. *Journal of Biological Chemistry* **274**: 37538-37543

Kinoshita E, Kinoshita-Kikuta E, Koike T (2015) Advances in Phos-tag-based methodologies for separation and detection of the phosphoproteome. *Biochimica et Biophysica Acta (BBA) - Proteins and Proteomics* **1854**: 601-608

Kinoshita E, Kinoshita-Kikuta E, Matsubara M, Aoki Y, Ohie S, Mouri Y, Koike T (2009) Two-dimensional phosphate-affinity gel electrophoresis for the analysis of phosphoprotein isotypes. *Electrophoresis* **30**: 550-559

Kleiman FE, Manley JL (2001) The BARD1-CstF-50 Interaction Links mRNA 3' End Formation to DNA Damage and Tumor Suppression. *Cell* **104**: 743-753

Kogoma T (1997) Stable DNA replication: interplay between DNA replication, homologous recombination, and transcription. *Microbiology and Molecular Biology Reviews* **61**: 212-238

Krajewska M, Fehrmann RS, de Vries EG, van Vugt MA (2015) Regulators of homologous recombination repair as novel targets for cancer treatment. *Frontiers in Genetics* **6**

Kuo LJ, Yang LX (2008) Gamma-H2AX - a novel biomarker for DNA double-strand breaks. *In Vivo* **22**: 305-309

Lavin MF, Kozlov S, Gatei M, Kijas AW (2015) ATM-Dependent Phosphorylation of All Three Members of the MRN Complex: From Sensor to Adaptor. *Biomolecules* **5**: 2877-2902

Leaw CL, Ren EC, Choong ML (2004) Hcc-1 is a novel component of the nuclear matrix with growth inhibitory function. *Cellular and Molecular Life Sciences* **61**: 2264-2273

Li M, Zhang P (2009) *Spindle assembly checkpoint, aneuploidy and tumorigenesis*: Cell Cycle. 2009 Nov 1;8(21):3440. Epub 2009 Dec 1.

Li X, Manley JL (2005) Inactivation of the SR protein splicing factor ASF/SF2 results in genomic instability. *Cell* **122**: 365-378

Lieber MR (2010) The mechanism of double-strand DNA break repair by the nonhomologous DNA end-joining pathway. *Annual Review of Biochemistry* **79**: 181-211

Lingle WL, Lutz WH, Ingle JN, Maihle NJ, Salisbury JL (1998) Centrosome hypertrophy in human breast tumors: implications for genomic stability and cell polarity. *Proceedings of the National Academy of Sciences of the United States of America* **95**: 2950-2955

Litvak V, Argov R, Dahan N, Ramachandran S, Amarilio R, Shainskaya A, Lev S (2004) Mitotic phosphorylation of the peripheral Golgi protein Nir2 by Cdk1 provides a docking mechanism for Plk1 and affects cytokinesis completion. *Molecular Cell* **14**: 319-330

Liu LF, Desai SD, Li T-K, Mao Y, Sun MEI, Sim S-P (2000) Mechanism of Action of Camptothecin. *Annals of the New York Academy of Sciences* **922**: 1-10

Luna R, Gaillard H, González-Aguilera C, Aguilera A (2008) Biogenesis of mRNPs: integrating different processes in the eukaryotic nucleus. *Chromosoma* **117**: 319-331

Luna R, Jimeno S, Marin M, Huertas P, Garcia-Rubio M, Aguilera A (2005) Interdependence between transcription and mRNP processing and export, and its impact on genetic stability. *Molecular Cell* **18**: 711-722

Mali P, Esvelt KM, Church GM (2013) Cas9 as a versatile tool for engineering biology. *Nature Methods* **10**: 957-963

Maréchal A, Li J-M, Ji XY, Wu C-S, Yazinski SA, Nguyen HD, Liu S, Jiménez AE, Jin J, Zou L (2014) PRP19 Transforms into a Sensor of RPA-ssDNA after DNA Damage and Drives ATR Activation via a Ubiquitin-Mediated Circuitry. *Molecular Cell* **53**: 235-246

Marechal A, Zou L (2013) DNA damage sensing by the ATM and ATR kinases. *Cold Spring Harbour Perspectives in Biology* **5**

Matsuoka S, Ballif BA, Smogorzewska A, McDonald ER, 3rd, Hurov KE, Luo J, Bakalarski CE, Zhao Z, Solimini N, Lerenthal Y, Shiloh Y, Gygi SP, Elledge SJ (2007) ATM and ATR substrate analysis reveals extensive protein networks responsive to DNA damage. *Science* **316**: 1160-1166

Matsuoka S, Huang M, Elledge SJ (1998) Linkage of ATM to cell cycle regulation by the Chk2 protein kinase. *Science* **282**: 1893-1897

Mayne LV, Lehmann AR (1982) Failure of RNA synthesis to recover after UV irradiation: an early defect in cells from individuals with Cockayne's syndrome and xeroderma pigmentosum. *Cancer Research* **42**: 1473-1478

McNulty DE, Annan RS (2008) Hydrophilic interaction chromatography reduces the complexity of the phosphoproteome and improves global phosphopeptide isolation and detection. *Molecular and Cellular Proteomics* **7**: 971-980

Mills KD, Ferguson DO, Alt FW (2003) The role of DNA breaks in genomic instability and tumorigenesis. *Immunological Reviews* **194**: 77-95

Minoshima Y, Kawashima T, Hirose K, Tonozuka Y, Kawajiri A, Bao YC, Deng X, Tatsuka M, Narumiya S, May WS, Jr., Nosaka T, Semba K, Inoue T, Satoh T, Inagaki M, Kitamura T (2003) Phosphorylation by aurora B converts MgcRacGAP to a RhoGAP during cytokinesis. *Developmental Cell* **4**: 549-560

Mishima M, Pavicic V, Gruneberg U, Nigg EA, Glotzer M (2004) Cell cycle regulation of central spindle assembly. *Nature* **430**: 908-913

Mollinari C, Kleman J-P, Jiang W, Schoehn G, Hunter T, Margolis RL (2002) PRC1 is a microtubule binding and bundling protein essential to maintain the mitotic spindle midzone. *The Journal of Cell Biology* **157**: 1175-1186

Montecucco A, Biamonti G (2013) Pre-mRNA processing factors meet the DNA damage response. *Frontiers in Genetics* **4**: 102

Murnane JP (2006) Telomeres and chromosome instability. *DNA Repair* **5**: 1082-1092

Naro C, Bielli P, Pagliarini V, Sette C (2015) The interplay between DNA damage response and RNA processing: the unexpected role of splicing factors as gatekeepers of genome stability. *Frontiers in Genetics* **6**: 142

Neef R, Preisinger C, Sutcliffe J, Kopajtich R, Nigg EA, Mayer TU, Barr FA (2003) Phosphorylation of mitotic kinesin-like protein 2 by polo-like kinase 1 is required for cytokinesis. *The Journal of Cell Biology* **162**: 863-876

Nishino M, Kurasawa Y, Evans R, Lin SH, Brinkley BR, Yu-Lee LY (2006) NudC is required for Plk1 targeting to the kinetochore and chromosome congression. *Current Biology* **16**: 1414-1421

Normand G, King RW (2010) Understanding Cytokinesis Failure. *Advances in experimental medicine and biology* **676**: 27-55

Olsen JV, Vermeulen M, Santamaria A, Kumar C, Miller ML, Jensen LJ, Gnad F, Cox J, Jensen TS, Nigg EA, Brunak S, Mann M (2010) Quantitative phosphoproteomics reveals widespread full phosphorylation site occupancy during mitosis. *Science Signaling* **3**: 2000475

Onn I, Heidinger-Pauli JM, Guacci V, Ünal E, Koshland DE (2008) Sister Chromatid Cohesion: A Simple Concept with a Complex Reality. *Annual Review of Cell and Developmental Biology* **24**: 105-129

Paques F, Haber JE (1999) Multiple pathways of recombination induced by double-strand breaks in *Saccharomyces cerevisiae*. *Microbiology and Molecular Biology Reviews* **63**: 349-404

Paronetto MP, Minana B, Valcarcel J (2011) The Ewing sarcoma protein regulates DNA damage-induced alternative splicing. *Molecular Cell* **43**: 353-368

Paull TT (2015) Mechanisms of ATM Activation. *Annual Review of Biochemistry* **84**: 711-738

Paulsen RD, Soni DV, Wollman R, Hahn AT, Yee MC, Guan A, Hesley JA, Miller SC, Cromwell EF, Solow-Cordero DE, Meyer T, Cimprich KA (2009) A genome-wide siRNA screen reveals

diverse cellular processes and pathways that mediate genome stability. *Molecular Cell* **35**: 228-239

Peddibhotla S, Lam MH, Gonzalez-Rimbau M, Rosen JM (2009) The DNA-damage effector checkpoint kinase 1 is essential for chromosome segregation and cytokinesis. *Proceedings of the National Academy of Sciences of the United States of America* **106**: 5159-5164

Peterson ME, Chen F, Saven JG, Roos DS, Babbitt PC, Sali A (2009) Evolutionary constraints on structural similarity in orthologs and paralogs. *Protein Science* **18**: 1306-1315

Polo SE, Blackford AN, Chapman JR, Baskcomb L, Gravel S, Rusch A, Thomas A, Blundred R, Smith P, Kzhyshkowska J, Dobner T, Taylor AM, Turnell AS, Stewart GS, Grand RJ, Jackson SP (2012) Regulation of DNA-end resection by hnRNPU-like proteins promotes DNA double-strand break signaling and repair. *Mol Cell* **45**: 505-516

Richter H, Randau L, Plagens A (2013) Exploiting CRISPR/Cas: interference mechanisms and applications. *International Journal of Molecular Sciences* **14**: 14518-14531

Rogakou EP, Pilch DR, Orr AH, Ivanova VS, Bonner WM (1998) DNA double-stranded breaks induce histone H2AX phosphorylation on serine 139. *Journal of Biological Chemistry* **273**: 5858-5868

Roos WP, Kaina B (2013) DNA damage-induced cell death: From specific DNA lesions to the DNA damage response and apoptosis. *Cancer Letters* **332**: 237-248

Rosonina E, Kaneko S, Manley JL (2006) Terminating the transcript: breaking up is hard to do. *Genes and Development* **20**: 1050-1056

Roux KJ, Kim DI, Raida M, Burke B (2012) A promiscuous biotin ligase fusion protein identifies proximal and interacting proteins in mammalian cells. *The Journal of Cell Biology* **196**: 801-810

Rupnik A, Lowndes NF, Grenon M (2010) MRN and the race to the break. *Chromosoma* **119**: 115-135

Sage E, Harrison L (2011) Clustered DNA lesion repair in eukaryotes: relevance to mutagenesis and cell survival. *Mutation Research* **711**: 123-133

Santos-Pereira JM, Herrero AB, Moreno S, Aguilera A (2014) Npl3, a new link between RNA-binding proteins and the maintenance of genome integrity. *Cell Cycle* **13**: 1524-1529

Sarkaria JN, Busby EC, Tibbetts RS, Roos P, Taya Y, Karnitz LM, Abraham RT (1999) Inhibition of ATM and ATR kinase activities by the radiosensitizing agent, caffeine. *Cancer Research* **59**: 4375-4382

Sato N, Mizumoto K, Nakamura M, Nakamura K, Kusumoto M, Niiyama H, Ogawa T, Tanaka M (1999) Centrosome abnormalities in pancreatic ductal carcinoma. *Clinical Cancer Research* **5**: 963-970

Saunders A, Core LJ, Lis JT (2006) Breaking barriers to transcription elongation. *Nature Reviews Molecular Cell Biology* **7**: 557-567

Savage K, Harkin DP (2009) BRCA1 and BRCA2: Role in the DNA Damage Response, Cancer Formation and Treatment. In *The DNA Damage Response: Implications on Cancer Formation and Treatment*, Khanna KK, Shiloh Y (eds), pp 415-443. Dordrecht: Springer Netherlands

Savage Kienan I, Gorski Julia J, Barros Eliana M, Irwin Gareth W, Manti L, Powell Alexander J, Pellagatti A, Lukashchuk N, McCance Dennis J, McCluggage WG, Schettino G, Salto-Tellez M, Boulwood J, Richard Derek J, McDade Simon S, Harkin DP (2014) Identification of a BRCA1-mRNA Splicing Complex Required for Efficient DNA Repair and Maintenance of Genomic Stability. *Molecular Cell* **54**: 445-459

Schwab Rebekka A, Nieminuszczy J, Shah F, Langton J, Lopez Martinez D, Liang C-C, Cohn Martin A, Gibbons Richard J, Deans Andrew J, Niedzwiedz W (2015) The Fanconi Anemia Pathway Maintains Genome Stability by Coordinating Replication and Transcription. *Molecular Cell* **60**: 351-361

Shen Z (2011) Genomic instability and cancer: an introduction. *Journal of Molecular Cell Biology* **3**: 1-3

Shiloh Y (2003) ATM and related protein kinases: safeguarding genome integrity. *Nature Reviews Cancer* **3**: 155-168

Skourti-Stathaki K, Kamieniarz-Gdula K, Proudfoot NJ (2014) R-loops induce repressive chromatin marks over mammalian gene terminators. *Nature* **516**: 436-439

Smith E, Dejsuphong D, Balestrini A, Hampel M, Lenz C, Takeda S, Vindigni A, Costanzo V (2009) An ATM- and ATR-dependent checkpoint inactivates spindle assembly by targeting CEP63. *Nature Cell Biology* **11**: 278-285

Smith SL, Bowers NL, Betticher DC, Gautschi O, Ratschiller D, Hoban PR, Booton R, Santibáñez-Koref MF, Heighway J (2005) Overexpression of aurora B kinase (AURKB) in primary non-small cell lung carcinoma is frequent, generally driven from one allele, and correlates with the level of genetic instability. *British Journal of Cancer* **93**: 719-729

Sollier J, Stork CT, García-Rubio ML, Paulsen RD, Aguilera A, Cimprich KA (2014) Transcription-Coupled Nucleotide Excision Repair Factors Promote R-Loop-Induced Genome Instability. *Molecular Cell* **56**: 777-785

Sorrentino R, Libertini S, Pallante PL, Troncone G, Palombini L, Bavetsias V, Spalletti-Cernia D, Laccetti P, Linardopoulos S, Chieffi P, Fusco A, Portella G (2005) Aurora B overexpression associates with the thyroid carcinoma undifferentiated phenotype and is required for thyroid carcinoma cell proliferation. *Journal of Clinical Endocrinology and Metabolism* **90**: 928-935

Steigemann P, Wurzenberger C, Schmitz MH, Held M, Guizetti J, Maar S, Gerlich DW (2009) Aurora B-mediated abscission checkpoint protects against tetraploidization. *Cell* **136**: 473-484

Stilmann M, Hinz M, Arslan SC, Zimmer A, Schreiber V, Scheidereit C (2009) A nuclear poly(ADP-ribose)-dependent signalosome confers DNA damage-induced I κ B kinase activation. *Molecular Cell* **36**: 365-378

Storchova Z, Pellman D (2004) From polyploidy to aneuploidy, genome instability and cancer. *Nature Reviews Molecular Cell Biology* **5**: 45-54

Strasser K, Masuda S, Mason P, Pfannstiel J, Oppizzi M, Rodriguez-Navarro S, Rondon AG, Aguilera A, Struhl K, Reed R, Hurt E (2002) TREX is a conserved complex coupling transcription with messenger RNA export. *Nature* **417**: 304-308

Strebhardt K, Ullrich A (2006) Targeting polo-like kinase 1 for cancer therapy. *Nature Reviews Cancer* **6**: 321-330

Sturzenegger A, Burdova K, Kanagaraj R, Levikova M, Pinto C, Cejka P, Janscak P (2014) DNA2 cooperates with the WRN and BLM RecQ helicases to mediate long-range DNA end resection in human cells. *Journal of Biological Chemistry* **289**: 27314-27326

Sugiura T, Sakurai K, Nagano Y (2007) Intracellular characterization of DDX39, a novel growth-associated RNA helicase. *Experimental Cell Research* **313**: 782-790

Tatsuka M, Katayama H, Ota T, Tanaka T, Odashima S, Suzuki F, Terada Y (1998) Multinuclearity and increased ploidy caused by overexpression of the aurora- and Ipl1-like midbody-associated protein mitotic kinase in human cancer cells. *Cancer Research* **58**: 4811-4816

Tatusov RL, Koonin EV, Lipman DJ (1997) A genomic perspective on protein families. *Science* **278**: 631-637

Terns MP, Terns RM (2011) CRISPR-based adaptive immune systems. *Current Opinion in Microbiology* **14**: 321-327

Tresini M, Warmerdam DO, Kolovos P, Snijder L, Vrouwe MG, Demmers JA, van IWF, Grosveld FG, Medema RH, Hoeijmakers JH, Mullenders LH, Vermeulen W, Marteijn JA (2015) The core spliceosome as target and effector of non-canonical ATM signalling. *Nature* **523**: 53-58

Umlauf D, Bonnet J, Waharte F, Fournier M, Stierle M, Fischer B, Brino L, Devys D, Tora L (2013) The human TREX-2 complex is stably associated with the nuclear pore basket. *Journal of Cell Science* **126**: 2656-2667

Wang W (2007) Emergence of a DNA-damage response network consisting of Fanconi anaemia and BRCA proteins. *Nature Reviews Genetics* **8**: 735-748

Ward JF, Blakely WF, Joner EI (1985) Mammalian cells are not killed by DNA single-strand breaks caused by hydroxyl radicals from hydrogen peroxide. *Radiation Research* **103**: 383-392

Weber RG, Bridger JM, Benner A, Weisenberger D, Ehemann V, Reifemberger G, Lichter P (1998) Centrosome amplification as a possible mechanism for numerical chromosome aberrations in cerebral primitive neuroectodermal tumors with TP53 mutations. *Cytogenetics and Cell Genetics* **83**: 266-269

Wellinger RE, Prado F, Aguilera A (2006) Replication fork progression is impaired by transcription in hyperrecombinant yeast cells lacking a functional THO complex. *Molecular Cell Biology* **26**: 3327-3334

Wickramasinghe Vihandha O, Savill Jane M, Chavali S, Jonsdottir Asta B, Rajendra E, Grüner T, Laskey Ronald A, Babu MM, Venkitaraman Ashok R (2013) Human Inositol Polyphosphate Multikinase Regulates Transcript-Selective Nuclear mRNA Export to Preserve Genome Integrity. *Molecular Cell* **51**: 737-750

Wickramasinghe VO, Venkitaraman AR (2016) RNA Processing and Genome Stability: Cause and Consequence. *Molecular Cell* **61**: 496-505

Yamamoto Y, Eguchi S, Junpei A, Nagao K, Sakano S, Furuya T, Oga A, Kawauchi S, Sasaki K, Matsuyama H (2009) Intercellular centrosome number is correlated with the copy number of chromosomes in bladder cancer. *Cancer Genetics and Cytogenetics* **191**: 38-42

Yamazaki T, Fujiwara N, Yukinaga H, Ebisuya M, Shiki T, Kurihara T, Kioka N, Kambe T, Nagao M, Nishida E, Masuda S (2010) The closely related RNA helicases, UAP56 and URH49,

preferentially form distinct mRNA export machineries and coordinately regulate mitotic progression. *Molecular Biology of the Cell* **21**: 2953-2965

Yüce Ö, Piekny A, Glotzer M (2005) An ECT2–centralspindlin complex regulates the localization and function of RhoA. *The Journal of Cell Biology* **170**: 571-582